FFI Norwegian Defence Research Establishment

23/01379

FFI-RAPPORT

Polycarbonate in transparent armour

– mechanical properties, ballistic performance and ageing behaviour

Bernt B. Johnsen
Stephen J. Cimpoeru [1]

[1] Defence Science and Technology Group, Australian Department of Defence

Polycarbonate in transparent armour – mechanical properties, ballistic performance and ageing behaviour

Bernt B. Johnsen
Stephen J. Cimpoeru [1]

Norwegian Defence Research Establishment (FFI)
[1] Defence Science and Technology Group, Australian Department of Defence 14 August 2023

Keywords
Militære kjøretøyer
Beskyttelse
Pansermateriale
Laminerte konstruksjoner
Polymere forbindelser

FFI report
23/01379

Project number
1680

Electronic ISBN
978-82-464-3486-5

Approvers
Morten Huseby, *Research Manager*
Halvor Ajer, *Director of Research*

The document is electronically approved and therefore has no handwritten signature.

Summary

Polycarbonate is an engineering plastic that is frequently used as a component in, or as a stand-alone, transparent armour for many military applications. One important application of polycarbonate is in transparent armour systems for front and side windows in military ground vehicles. Other examples are goggles, visors and ballistic shields for individual soldiers. All these different transparent armours are designed to provide ballistic protection against specific projectile and fragment threats.

Transparent armours on ground vehicles are made of layers of materials, each with very different physical properties and behaviours during ballistic impact, with the most common materials being glass and polycarbonate. These armour systems are designed to be transparent but still provide effective ballistic protection despite being constrained by factors such as final thickness, weight and cost. Polycarbonate is usually chosen as the backing layer, and its main role is to contain eroded projectiles and armour fragments.

This report gives an overview of the mechanical properties, ballistic performance and ageing behaviour of polycarbonate. Polycarbonate is a ductile material and the deformation behaviour of polycarbonate is similar to that of many engineering plastics. Several material properties are strain rate dependent, and there is some increase in the yield stress and hardening with increasing strain rate. Sheets that are impacted by projectiles will normally fail by plastic deformation, and several penetration mechanisms have been identified. Overall, thinner plates favour more extensive dishing of the target, while thicker plates may favour plugging failures more.

Although polycarbonate has some excellent properties that make it suitable for use in armour systems, it also has some major drawbacks. The material is known to degrade on a molecular level when exposed to ageing conditions, such as ultraviolet light, humidity and temperature, ultimately resulting in embrittlement and premature failure. In the ageing of transparent armour, both the degradation of the polycarbonate (critical for the ballistic performance), and also of the adhesive interlayers (critical to transparency), may contribute to the failure of the armour being unable to fulfil its role. Ageing results in the transparent armours having a lifetime that is much shorter than that of the vehicles, resulting in high replacement costs and significantly increased operational costs. These topics are addressed in this report.

Sammendrag

Polykarbonat er et plastmateriale som er mye brukt i ulike typer av gjennomsiktig ballistisk beskyttelse. Dette inkluderer også komponenter som inngår i mange militære beskyttelsessystemer. En viktig anvendelse er panserglass i frontruter og sidevinduer på militære kjøretøy. Andre anvendelser er beskyttelsesbriller, visir og skjold for soldater. Alle de gjennomsiktige beskyttelsessystemene er designet for å gi beskyttelse mot definerte trusler, som ulike kuler og fragmenter.

Panserglass på militære kjøretøy er bygget opp av flere lag av ulike materialer som har ulike materialegenskaper og ulik oppførsel under ballistisk anslag. De vanligste materialene er glass og polykarbonat. Panserglassene er gjennomsiktige, men gir effektiv beskyttelse selv om faktorer som tykkelse, vekt og kostnad legger begrensninger på designet. Det bakerste laget i panserglasset er vanligvis polykarbonat, siden polykarbonat er relativt duktilt og i stand til å fange opp restenergien fra eroderte prosjektiler og andre materialfragmenter.

Denne rapporten gir en oversikt over de mekaniske egenskapene, den ballistiske ytelsen og aldring av polykarbonat. Siden polykarbonat er et duktilt materiale vil det deformeres på samme måte som mange andre plastmaterialer. Dette betyr også at flere materialparametere er hastighetsavhengige – blant annet vil styrken øke ved økende deformasjonshastighet. Den dominerende deformasjonsmekanismen under ballistisk anslag fra prosjektiler, avhenger i stor grad av tykkelsen til polykarbonatplaten. Materialet vil vanligvis gjennomgå plastisk deformasjon, og flere ulike penetrasjonsmekanismer kan finne sted.

Selv om polykarbonat har noen gode egenskaper som gjør at det er godt egnet til bruk i beskyttelsessystemer, så har materialet også noen ulemper. Det er velkjent at polykarbonat kan degraderes når det blir utsatt ulike miljøpåvirkninger som ultrafiolett lys, høy fuktighet og høy temperatur. Dette kan gjøre materialet mer sprøtt og resulterer i lavere ytelse. I panserglass for kjøretøy vil også degradering av limfugen mellom de ulike lagene i strukturen være av avgjørende betydning. Dersom limfugen degraderes vil panserglasset kunne bli mindre gjennomsiktig. Miljøpåvirkninger vil dermed kunne medføre at levetiden til panserglass på kjøretøy blir mye kortere enn forventet, noe som gir betydelig økte utgifter til oppgradering og vedlikehold. Disse temaene er belyst i denne rapporten.

Contents

Preface

This report was written in a collaborative effort between the Norwegian Defence Research Establishment, Norway, and the Defence Science and Technology Group, Australia.

The authors would like to thank the quoted presenters at the Workshop on ageing effects in protective systems, components and materials, held at ISL, Saint-Louis, France in 2017, 2018 2019 and 2022, for giving permission to quote their work.

Kjeller, 14 August 2023
Bernt B. Johnsen

1 Introduction

Transparent armour on ground vehicles and aircraft is an armour system consisting of different transparent materials, which is designed to provide ballistic protection against projectiles and fragments. Transparent materials such as glass, glass ceramics, ceramics and engineering plastics can have very different physical properties, and can behave very differently both during ballistic impact and during their service lives. In transparent armour they are combined in a layered structure that is optimised with respect to ballistic performance, weight and cost. Some examples of transparent armour on military vehicles are shown in Figure 1.1.

Front window on the Thales Bushmaster Side window on the Oshkosh M-ATV

Figure 1.1 Transparent armour on armoured vehicles [1].

Transparent armour is a system that is usually constructed with a hard strike face and a more ductile backing layer. When impacted by a projectile, the hard strike face break up and/or erode the projectile, while the main role of the backing layer is to catch the residual fragments from the projectile and the harder front layers, and prevent them from perforating the armour. For transparent armour, the strike face is often made of glass and the ductile backing of an engineering plastic. The glass then erodes the projectiles, while the plastic backing catches the debris.

Compared to opaque armours, transparent armour will always substantially underperform in ballistic performance for a given threat condition, including space efficiency and weight efficiency. This simply because the transparent materials normally used for its construction do not have comparable mechanical properties to conventional armour materials. Transparent armours usually have substantially less multi-hit capability than opaque armours and would be expected to be penetrated when the minimum shot-to-shot impact spacing is exceeded. Visibility through transparent armour is also considerably reduced after ballistic impact, Figure 1.2.

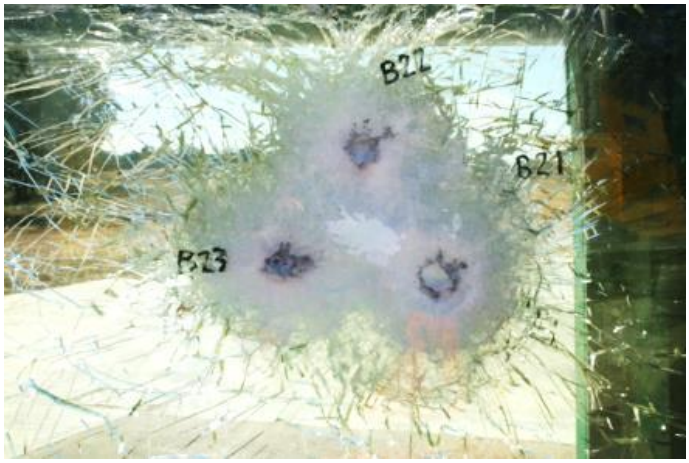

Figure 1.2 Transparent armour impacted by multiple ballistic impacts at a minimum shot-to-shot impact spacing. Reproduced from Yang et al. [2].

Hence, affordable transparent armour is a challenging problem for military vehicles. Not just because of performance, weight and cost issues but for a host of other functional requirements, which include:

- Multi-hit capability
- Optical distortion, including meeting automotive design standards
- Temperature dependence of ballistic performance
- Light transmission
- Signature management
- Laser protection
- Environmental durability
- Armour service life

While transparent armour is a complex armour system where performance is dependent on many factors, such as the glass on the impact face and adhesive interlayers that join the component parts together, the polymer backing layer has increasingly been identified to be of specific importance to the performance and durability of the system.

The polymer backing layer is usually polycarbonate (PC). PC is an engineering plastic that is used as a component of (or as stand-alone) transparent armour in many military and civilian applications. Examples of the use PC is wide, and it is used in goggles, spectacles, visors, face shields for personnel, ballistic shields, and for protection of occupants in ground and air vehicles, of which the use of PC in transparent armour systems for windshields and side-windows in military ground vehicles is the most extensive. An even more sophisticated application of PC is in astronaut helmets and visors to protect the wearer from various hazards. The main reason for the use of PC in these applications is its impact resistance and excellent transparency [3-8].

Although PC has some excellent properties that makes it suitable for use in transparent systems for ballistic protection, it also has some major drawbacks. For one, it has relatively low scratch or abrasion resistance compared to other engineering plastics, but this can often be solved by the application of hard surface coatings. PC is also known to degrade when exposed to environmental conditions, such as ultraviolet (UV) light, humidity and temperature. For this reason, components that include PC may experience reduced ballistic performance after a period in service. However, the actual effect of ageing on the ballistic protective capability of PC is not well documented in the open literature.

This report gives an overview of the literature on PC with specific emphasis on its mechanical properties, ballistic performance and ageing behaviour. With respect to mechanical properties, the main focus will be on tension and compression tests, since these are relatively simple tests. Particular focus will also be given to the use of PC as a component of transparent armour for vehicles, as well as the ageing behaviour of these systems. In these armour systems, the adhesive interlayer between laminates may also be affected, in addition to ageing of the PC itself.

2 Transparent armour in ground vehicles

The main role of the transparent armour on military ground vehicles is to provide ballistic protection against projectiles and fragments, while at the same time providing high levels of optical transparency for the occupants. The windows in ground vehicles are designed to protect against ball or armour piercing threats, as well as high-velocity fragments, and they must be able to withstand multiple hits and to fracture in a way that maintains their structural integrity and maintains a minimum level of transparency. To achieve this, the transparent armour is constructed as a layered system of transparent materials, where each layer has a slightly different function. This was thoroughly described by Grujicic et al. [6], and a good introduction to transparent armour can be found in a report from the National Academy of Sciences [9]. Excellent overviews of the use of transparent armour, and of the materials that are employed in transparent armour, are also given in two articles by Patel et al. [4] and Sands et al. [5], both of the U.S. Army Research Laboratory.

2.1 Design and materials

Transparent armour systems for ground vehicles typically consist of three functional layers: (i) a hard strike face that gives erosion and fragmentation of the projectile, (ii) an intermediate layer with energy-absorbing properties, and (iii) a backing layer for containment of fragmented armour and projectile debris [6, 9]. However, several different designs exist. This is illustrated in Figure 2.1, where both traditional and newer designs of transparent armour are shown. The strike face is typically made of glass but glass-ceramic or transparent ceramics have also been used for specific applications.

Most transparent armours consist of multiple layers of soda lime or borosilicate glass. These can be produced by the relatively inexpensive float glass process. Borosilicate glass is more specialised and more difficult to produce but provides an approximate 10% weight saving compared to soda lime glass. It is affordable though still expensive. Other designs use glass ceramics. These are derived from kitchen cooktop materials and are glass-based materials where ceramic nanocrystallites are embedded in an amorphous silica matrix. They have improved ballistic performance compared with traditional glass, and while not inexpensive they have been used in military vehicles, for example the U.S. Army M-ATV[1]. Another option are transparent ceramics. They are harder, stronger, and tougher than traditional glass, and provide superior ballistic protection. The three most common types of transparent ceramics are aluminium oxynitride (AlON), magnesium aluminate ($MgAl_2O_4$, spinel), and single-crystal aluminium oxide (Al_2O_3, sapphire), each with different advantages and disadvantages. However, their use is severely limited by their extremely high cost, limited production capacity and limited sizes available. An overview of many glasses and ceramics used in transparent armour was given by Crouch et al. [10].

[1] M-ATV; MRAP All-Terrain Vehicle (MRAP; Mine Resistant Ambush Protected).

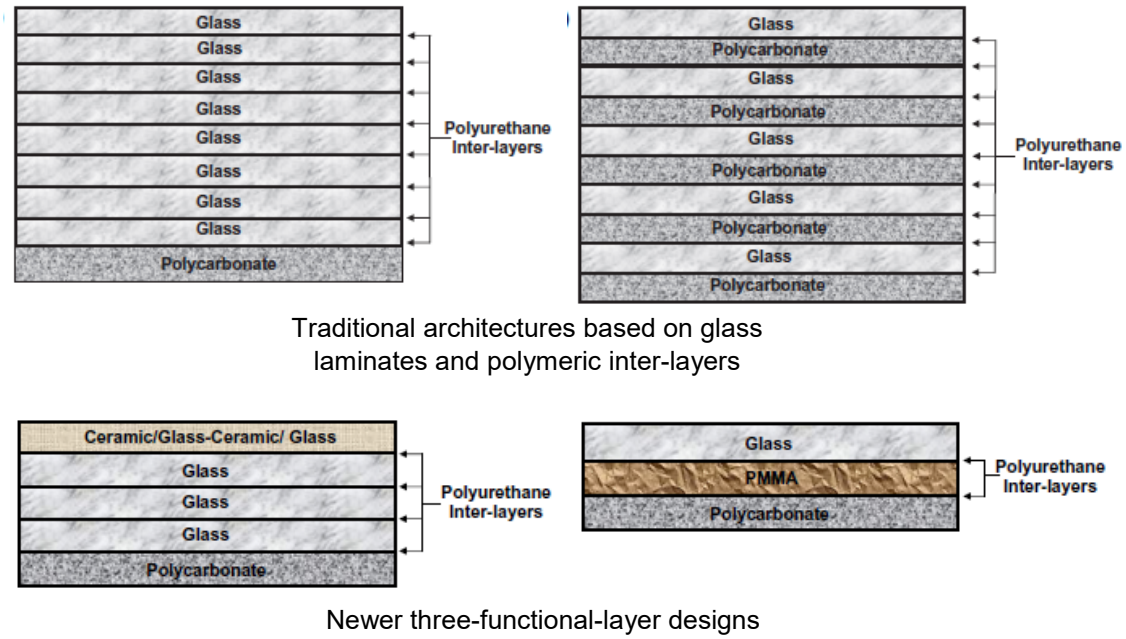

Figure 2.1 *Design of transparent armour systems. Reproduced with permission from Grujicic et al. [6].*

Intermediate transparent layers are typically made of glass or polymethylmethacrylate (PMMA), while the backing layer is usually made of PC. Common for all layered components is that they have high optical transparency in the visible and infrared wavelength ranges, and the selection of the different materials represent a trade-off between cost and performance. Most transparent armour also have thin adhesive inter-layers, typically consisting of polyurethane (PU) or alternatively polyvinyl butyral (PVB), adhesives whose main purpose whilst maintaining optical transparency is to join the different layers, mitigate thermal expansion mismatch and contain ballistic damage when impacted.

2.2 Protective capability

Transparent armour on ground vehicles must be able to withstand multiple hits since most threat weapons are typically automatic or semiautomatic and opposing forces will often fire at what they can see through the vehicle windows. However, with an areal density around 250-270 kg/m^2, laminated glass windows may impose a serious weight penalty [9]. For example, windows for Humvee vehicles in the U.S. Army are about 10 cm thick and weigh about 40 kg each. Six windows on a typical vehicle therefore adds considerable weight. This weight penalty may pose a significant disadvantage. If considering an add-on armour on vehicles, the transparent armour may cover only 15% of the total area, but contribute to 30% of the weight [5]. The extra window weight on the vehicle may contribute to a required upgrade or wear of the transmission and suspension systems. A reduction in window area is usually not realistic, since

the windows must be designed so that the driver's field of view is not obstructed. The thickness of the armour may also take up volume inside the cabin but it can also be fitted externally. Another significant drawback is the high cost and weight of the armour. There is therefore a drive towards developing thinner, lighter, and more cost-efficient transparent armour systems.

Strassburger [11] demonstrated possible weight savings by using transparent ceramics, such as AlON, spinel and sapphire, in laminated systems. An armour piercing 7.62 mm P80 projectile was defeated by a float-glass/PC armour with an areal density of ~170 kg/m^2, but the same effect was seen for targets of areal density ~60 kg/m^2 when the transparent ceramics were employed. However, the challenges with more cost-effective materials and larger, shapeable sizes still remain. Other examples of the protection offered by transparent armour were given by Crouch et al. [10].

The requirements for aircraft are similar to ground vehicles, and the armour systems are often designed to protect against 7.62 mm and 12.7 mm projectiles, as well as 23 mm High Explosive Incendiary (HEI) threats [5]. US development programmes have had the goal of developing transparent armour with an areal density of no more than 26.9 kg/m^2 for protection against the 7.62 mm PS Ball threat with a minimum of 90% light transmission [5]. Another goal was to defeat the blast and fragments from a 23 mm HEI projectile at a detonation distance of 4.3 m with an armour areal density of maximum 29.3 kg/m^2.

3 Polycarbonate in transparent armour

3.1 Polymer materials

Amorphous, glassy polymers are used in a wide variety of transparent armour where high visual transmittance is a requirement [5]. Based on their physical and thermo-mechanical properties the polymers are classified as thermoplastics or thermosets. Thermoplastics are linear polymers that become soft and deformable upon heating. This means they can be formed into different shapes without altering the properties of the polymer. End products from thermoplastics can be produced by extrusion moulding or injection moulding at elevated process temperatures. Thermosets, on the other hand, are cross-linked polymers that have very limited flow under elevated temperature. Products of thermosets are often manufactured by casting processes, and the finished materials cannot be reshaped at elevated temperatures. The physical properties of polymers vary significantly with temperature and deformation rate. Above the glass transition temperature (T_g), the polymer will change from a rigid to a more rubber-like structure due to thermal molecular motions, hence the T_g is indicative of the upper limit for the service temperature of the polymer.

The three most common polymers in transparent armour are polycarbonate, polymethylmethacrylate and polyurethane [4-6]. Thermoplastic PC is the most common, but thermoplastic PMMA has found widespread use in specialised applications such as periscopes. PMMA has many desirable properties, like high impact resistance, but it is nevertheless brittle. PC, on the other hand, is a ductile material that absorbs the impact energy by different deformation and failure mechanisms compared with PMMA. It offers excellent protection against smaller fragments, and it is the preferred material in applications where impact toughness is more critical. Thermoset PU is a transparent polymer that can be tailored to be rigid and brittle, like a glass, or flexible and ductile like an elastomer. Some formulations of PU have shown promising ballistic performance and are becoming increasingly used in some transparent armour applications.

Typical material properties for commercial polymers used in ballistic protection applications are given in Table 3.1. As PC is the most common transparent polymer used for transparent armour applications, it was chosen as the subject for of the present review.

Table 3.1 A comparison of typical properties of polymer materials found in transparent armour systems [5, 6, 12].

Property	Units	Lexan polycarbonate[2]	Simula, Inc., polyurethane	Plexi glass G PMMA
Density	kg/m^3	1200	1104	1190
Areal density at 25.4 mm thickness	kg/m^2	30.3	27.8	30.3
Tensile strength	MPa	66	62	72
Tensile modulus	MPa	2208	689	3102
Shear strength	MPa	45	--	62
Shear modulus	MPa	1000	--	1151
Compressive strength	MPa	83	72	124
Compressive modulus	MPa	1660	1241	3030
Flexural strength	MPa	104	89	104
Flexural modulus	MPa	2586	2020	3280
Max. operating temperature	°C	121	149	95
Glass transition temperature (T_g)	°C	145	-75	100
Manufacturing process		Extrusion and injection moulding	Casting and liquid injection moulding	Casting and later thermoforming
Main limitations		Degradation from chemical, UV-irradiation, scratches, abrasion	Slight tinting in thicker sections	Relatively brittle

[2] Other typical properties for PC: tensile elongation at break 90-120%, Poisson's ratio 0.37, Rockwell hardness M 70-80, transmittance 84-90%, speed of sound 2270 m/s, water absorption 0.16-0.35%, β-relaxation temperature (T_β) around -60ºC.

3.2 Polycarbonate

By itself PC offers excellent protection against small, low energy fragments, and as mentioned above, has found widespread use in applications such as goggles, visors, and as backing layer in transparent armour systems for vehicles. PC is employed in the backing layer, or spall layer, in transparent armour mainly because its excellent in-plane and through-thickness ductility facilitate the formation of a ductile failure mechanism rather than a low-energy brittle failure mechanism. While the backing does not play a major role in defeating the projectile, its main role is to contain the eroded projectile and armour fragments, including glass debris. Although PC has been found to be effective as thinner sheets as part of a transparent armour system, its use in thick sections is less efficient.

Since PC is an amorphous, thermoplastic polymer it can be moulded and shaped without degradation of the molecular structure. The structure of the repeating unit of bisphenol-A polycarbonate is shown in Figure 3.1. The amorphous polymer has a glass transition temperature which is well above room temperature at around 147°C. The value of the T_g means that processed PC can be exposed to relatively high temperatures, over shorter periods of time, without significant changes in the material properties.

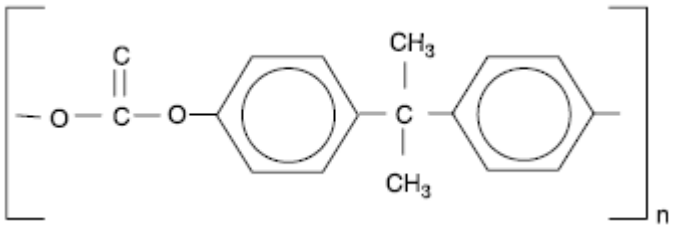

Figure 3.1 The structure of bisphenol-A polycarbonate.

The properties and the ballistic resistance of PC were compared with many other polymer materials by Henry [3]. In his paper, Henry quotes older work by Martin et al. [13], that was able to demonstrate a correlation between the spread between the thermal transition temperatures in polymers and their ballistic resistance. PC, like other polymers, has two thermal transition temperatures, the already mentioned T_g, and the secondary β-relaxation (T_β) at a lower temperature that relates to the motion of the main backbone chain in the polymer. It appears that the difference between these two transition temperatures has an effect on the ballistic properties of the polymer, with a larger difference believed to result in better ballistic performance (when comparing different polymers). Hence, the molecular structure of the main backbone chain of the polymer, which affects the stiffness of the polymer, was demonstrated to be much more important than different molecular orientations as the result of different processing conditions. It was also noted by Henry [3] that the secondary T_β transition contributes to the impact resistance

by dissipating impact energy via a large number of random thermal motions. A similar point was also made by Sands et al. [5], who stated that the ductility of PC is associated with molecular motion of the main chain molecules. The molecular motion is present even during high-rate impacts as well as at low temperatures. This mechanism contributes to sufficient energy dissipation and, as a result, the PC has excellent impact toughness over a wide temperature range.

3.3 In-service challenges

Despite its excellent properties that make PC suitable for use in backing layers in armour, it is well documented that transparent armour systems have a lifetime that is much shorter than opaque vehicle armour, see for example [6]. PC has limited ultraviolet (UV) radiation, chemical and scratch resistance. Hence, the use of UV-stabilizers and hard surface coatings is generally required. Nevertheless, embrittlement of the PC backing layer due to environmental degradation may still occur. Another limitation is physical ageing of PC, as the result of exposure to elevated temperature. Physical ageing is related to molecular motions in the glassy polymer, and results in stiffening and reduced impact properties of the material [14, 15]. Long-term exposure to elevated temperature will then cause the yield stress of a glassy polymer to increase, which will change the intrinsic behaviour of the polymer, and ultimately trigger a ductile-to-brittle transition. The overall effect this will have on the ballistic protection capability of the transparent armour system is not well known.

Another, perhaps more serious, problem is the loss of transparency caused by environmentally-induced delamination between the PC and the glass, and other factors such as abrasion or minor impact damage to the outer layer of the glass. Delamination interferes with visibility through the windows and such the transparent armour has to be replaced because it affects the ability of the crew, particularly the driver, to safely operate the vehicle. Though it is difficult to quantify, delamination may also reduce the ballistic performance of the armour. Reduced transparency due to delamination is a problem that needs to be seriously addressed because of the high ongoing replacement costs of transparent armour for military ground vehicles[3].

Hence, it emerges that two issues are of particular interest with respect to ageing of layered transparent armour systems: (i) delamination between laminates, i.e. usually between the intermediate layer(s) and the backing layer, and (ii) how ageing affects the properties of the PC laminate. Both these issues may affect the protective performance.

[3] Delamination can also lead to moisture ingress between layers, leading to fogging of the transparent armour with significantly reduced visibility; such transparent armour is normally being replaced before this stage is reached.

4 Mechanical behaviour of polycarbonate

4.1 Tension at quasi-static and higher strain rates

4.1.1 Quasi-static strain rates

There are several papers in the literature that have reported the tensile properties of polycarbonate at quasi-static and low rates, such as [16-26]. They all reported a similar deformation behaviour during the tensile testing, and several of these papers also reported results for higher strain rates. The quasi-static stress–strain response typically consists of a linear elastic and non-linear elastic deformation stages, a yield drop[4] from the initiation of necking and propagation of a necked region along the gauge length of a test specimen. Subsequent strain hardening has also been reported by some authors. A typical stress-strain curve for PC was presented by Hill et al. [27], Figure 4.1.

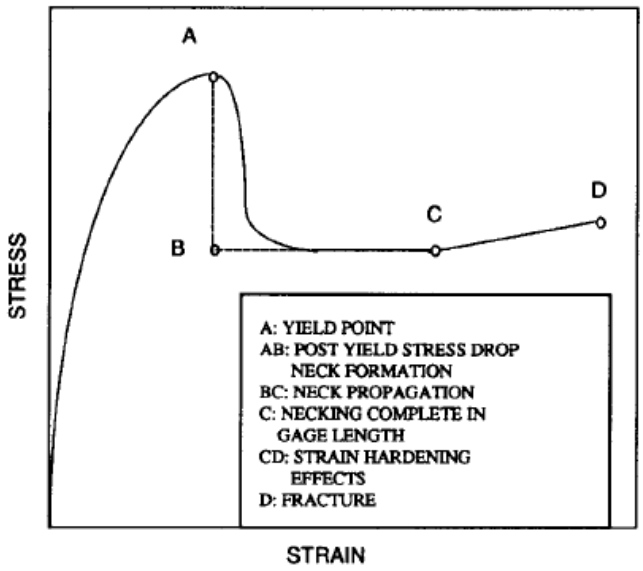

Figure 4.1 Typical tensile stress-strain curve for an extruded polycarbonate material. Reproduced with permission from Hill et al. [27].

The neck propagation in PC, as marked between point B and C in Figure 4.1, was reported in a study by Dwivedi et al. [18]. Neck propagation, which is also commonly referred to as drawing, initiates at the point where molecular orientation in the neck stiffens the polymer, and the polymer begins to extend by drawing fresh material from the tapering regions on either side of

[4] A yield drop due to necking is seen when engineering stress is graphed, but if true stress is plotted based on the actual cross-sectional area at the neck, there is no yield drop with only a short period of constant stress.

the initial neck [14]. Dwivedi et al. observed necking of cylindrical tensile specimens, Figure 4.2, corresponding to a relatively flat portion of the stress-strain curve between strains of 0.1 mm/mm and 0.4 mm/mm. At this strain, the cross-sectional area of the neck remains relatively constant, and there is no yield drop, only a period of constant stress. Once neck propagation had finished, the flow stress began to increase due to strain hardening, as illustrated between point C and D in Figure 4.1. The values of the mechanical properties were also similar to what has been reported in Table 3.1. Similar deformation behaviour and similar measured material properties have also been observed by Bauwens-Crowet et al. [19], Adam et al. [20] and Husain et al. [21]. A similar neck propagation for rectangular test specimens was illustrated by Cao et al. [23].

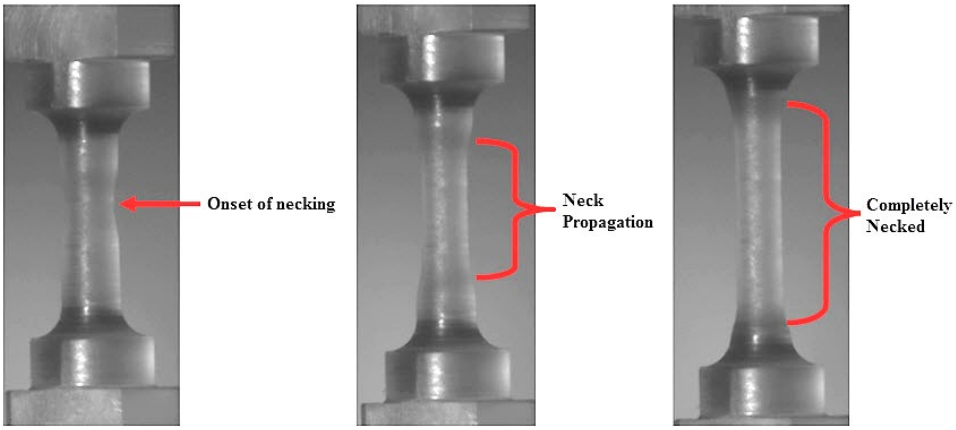

Figure 4.2 *Neck propagation during quasi-static tensile testing of cylindrical polycarbonate specimens. Reproduced from Dwiwedi et al. [18].*

Another example of tensile testing of PC was presented by Dekkers and Heinkens [16]. To reduce thermal stresses, the specimens were annealed at 80°C for 24 hours, then conditioned at 20°C and 55% relative humidity for at least 48 hours before testing. The tensile tests were performed at 20°C at a strain rate of 2.4 s^{-1}. The stress-strain curve had a peak stress followed by the formation of a distinct neck. The neck propagated through almost the entire gauge length until specimen failure at an elongation of around 100%. The yield stress was ~62 MPa at a yield strain of ~5.5%. Significant strain recovery was observed when unloading near (below) the yield point, and no stress-whitening or opacity was observed until the moment that necking commenced. The only significant non-Hookean deformation mechanism was shear deformation bands that formed in advance of the propagating neck.

4.1.2 Higher strain rates

Several authors have discussed the high rate properties of PC, where the tensile behaviour has been evaluated using the split Hopkinson tension bar (SHTB). For example, Cao et al. [23] and Fu et al. [25] have conducted studies that gave relatively similar results. The results clearly showed that the material behaviour of PC is strain rate dependent, and there is always an increase in the yield stress and yield strain with increasing strain rate.

Cao et al. [23] investigated the effect of strain rate on the tensile behaviour of PC under uniaxial tension loading conditions. The experiments were carried out using a conventional servo-hydraulic testing machine, a moderate strain-rate testing apparatus (the specimen was held in two grips and loaded by a hydraulic power unit) and a SHTB. Tensile stress–strain responses were obtained at various strain rates ranging from 0.001 s^{-1} to 1700 s^{-1}.

The experimental results showed that the tensile behaviour of the PC is sensitive to strain rate, which can be clearly seen from the results in Figure 4.3. The yield strength increases significantly with increasing strain rate and the dynamic yield strength is much greater than that under quasi-static loading conditions. At a strain rate of 0.001 s^{-1}, the peak stress was 64.7 MPa, which increased to 99.0 MPa at 1700 s^{-1}.

A viscoelastic constitutive model was proposed by Cao et al. [23] to describe the tensile stress–strain behaviour of PC prior to yielding. The model was capable of capturing the non-linear deformation characteristics of PC subjected to uniaxial tension loading over a wide range of strain rates.

The tensile behaviour of PC at both quasi-static and high strain-rate loading conditions was also investigated by Fu et al. [25]. Quasi-static testing was conducted at 0.001 and 0.05 s^{-1}, while the SHTB was employed for the dynamic strain rates of 380, 800 and 1750 s^{-1}. The geometry of the specimen was a dumb-bell shaped cylinder with a 4 mm diameter gauge section. All tests were conducted at room temperature.

The results showed that the quasi-static stress–strain response consisted of a linear elastic and non-linear elastic deformation stage, a yield drop and a necking propagation stage (typical tensile behaviour of PC as discussed above). Due to a limitation in the duration of the incident stress pulse, the entire deformation process after the peak strength could not be obtained in the dynamic tests. Nevertheless, the results indicated a definite rate dependence of the behaviour of PC, Figure 4.4, with both yield stress and yield strain increasing with increasing strain rate. The value of the yield stress under dynamic loading (around 95-105 MPa) was much greater than that under quasi-static loading (around 60-65 MPa). The strain rate dependence is very similar to that observed by Cao et al. [23].

The yield stress and yield strain were also modelled by Fu et al. [25] for a wide range of strain rates. The model results agreed well with the experimental data, as shown in Figure 4.4.

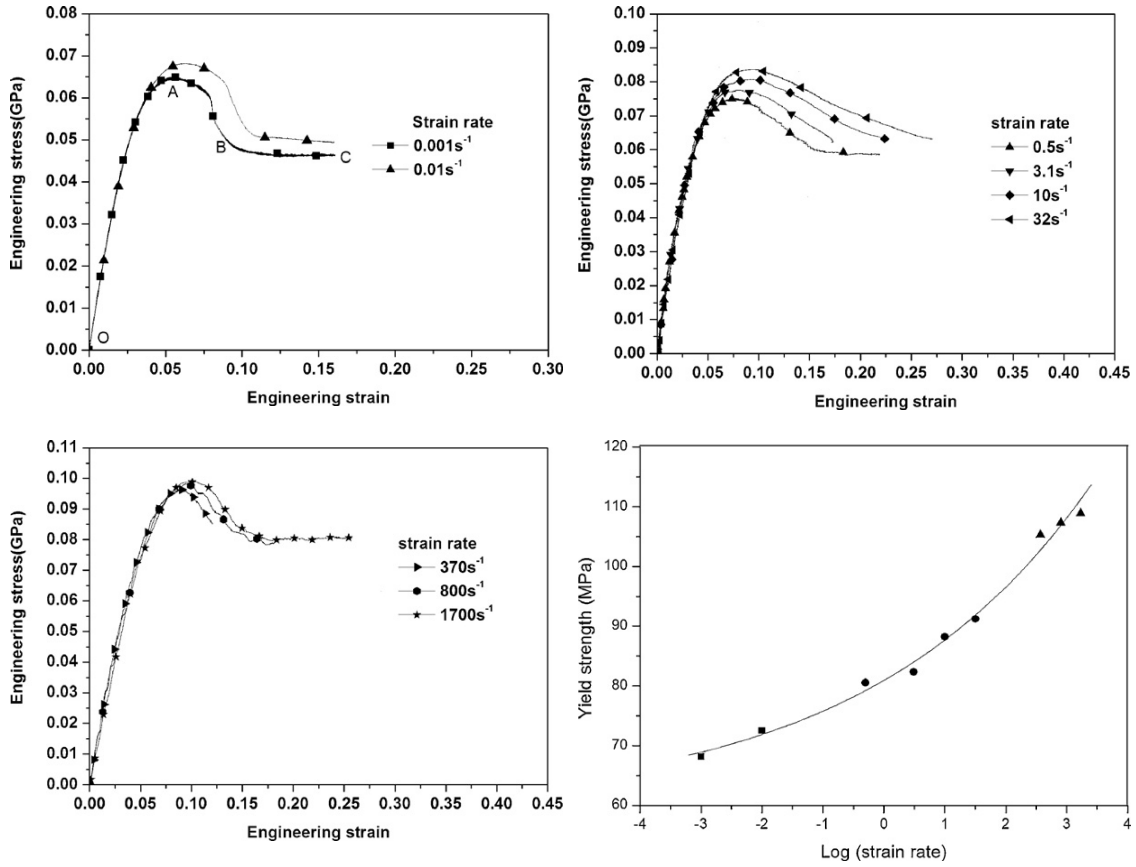

Figure 4.3 *Tensile stress–strain curves at various strain rates (top left to bottom left) and the variation of yield strength (peak stress) with respect to strain rate (bottom right). Reproduced with permission from Cao et al. [23].*

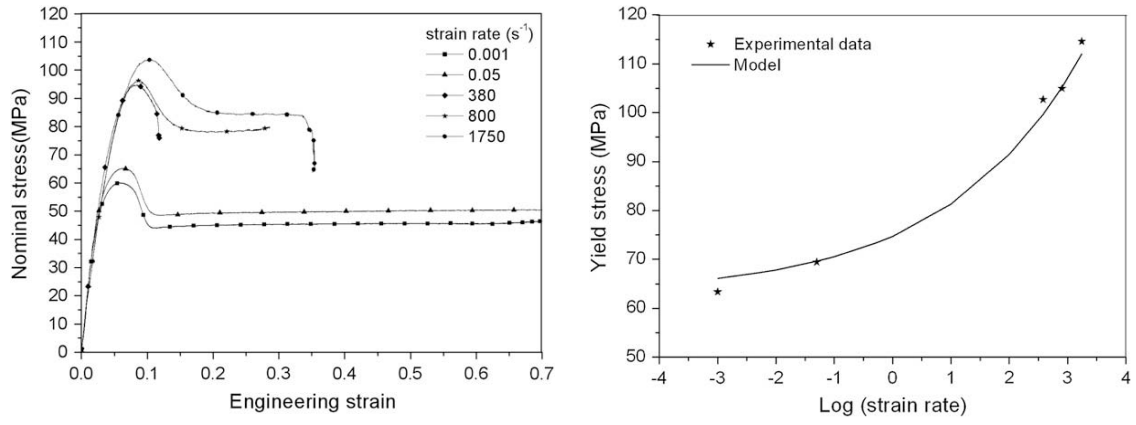

Figure 4.4 *Uniaxial tensile stress-strain curves at different strain rates (left), and tensile yield stress versus logarithmic strain rate (right). Reproduced with permission from Fu et al. [25].*

4.2 Compression at quasi-static and higher strain rates

The compressive material properties of PC at both quasi-static and higher strain rates have been reported in several papers in the literature. The compressive behaviour at high rates was determined by the split Hopkinson pressure bar (SHPB). It has been found that the material behaviour of PC in compression is strongly strain rate dependent, which is similar to the material behaviour in tension.

Compressive testing of PC at quasi-static rates have been conducted by authors such as Mulliken and Boyce [28], Siviour et al. [24], Dwivedi et al. [18], and Hahn and Herzig [26]. In compression, PC undergoes a linear elastic and non-linear elastic deformation stage, then a yield drop followed by strain hardening and failure. Compared to tension, a higher yield stress, no necking behaviour, and sometimes more dramatic strain hardening at lower strains, is observed in compression. The different strain hardening behaviour is caused by different molecular orientation taking place during tension and compression [22]. In tension, strain-induced alignment of polymer chains, where the molecular chains align uniaxially along the axis of elongation, is occurring, while in compression the chains align in a plane normal to axis of compression. This causes different material behaviour in tension and compression.

Dwivedi et al. [18] conducted both quasi-static and dynamic compression tests of PC. Specimens were machined from a 12.7 mm thick plate. The quasi-static compression tests were conducted at strain rates between 0.005 s^{-1} and 0.4 s^{-1}. High rate compression experiments were conducted using the SHPB at strain rates between 1750 s^{-1} and 15000 s^{-1}. (Tensile testing on the same PC material is described in Section 4.1.) The stress-strain curves at the quasi-static strain rates displayed similar behaviour. The peak strain was obtained at around 0.08 mm/mm strain, followed by strain softening and then strain hardening after a strain of around 0.3 mm/mm, Figure 4.5. The data suggested that the yield stress, and to a lesser extent the elastic modulus, correlated with strain rate.

Similar behaviour was observed in the high rate compression tests. However, the yield stress values were significantly higher, as shown in Figure 4.5. At some point between quasi-static and dynamic conditions, the strain rate effect on the apparent yield stress became more dramatic. Extrapolation of the data indicated that the material response is rate sensitive with enhanced hardening at rates greater than 10 s^{-1}. Others have reported the value to be closer to 100 s^{-1}, for example, Mulliken and Boyce [28] found a strain transition close to 150 s^{-1}, as explained below.

Additionally, testing at elevated temperatures caused a decrease in the yield and flow stresses at a strain rate of 0.005 s^{-1}. The yield strength decreased by almost 20 MPa when the temperature was increased from 22°C to 71°C. Similar behaviour was observed at the higher strain rate of 1800 s^{-1}, where the yield strength decreased by more than 15 MPa when the temperature was increased from 22°C to 54°C. (As mentioned below, a temperature dependency for PC was also observed by Siviour et al. [24].)

The experimental data were used by Dwivedi et al. [18] to determine parameters for the Johnson-Cook strength model and the Zerilli-Armstrong polymer strength model. Fits to the model data were shown to provide a reasonable approximation of real world behaviour.

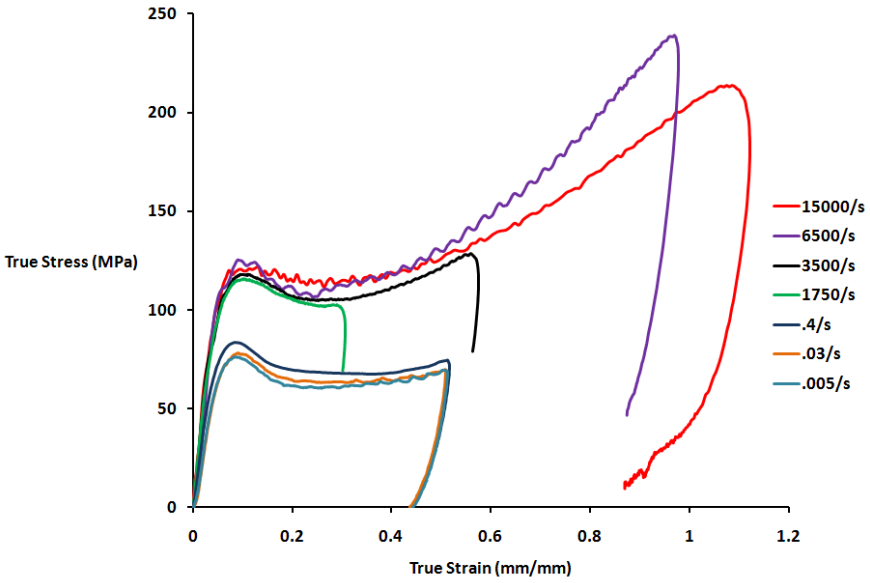

Figure 4.5 *Stress-strain curves from quasi-static and dynamic compression testing of polycarbonate. Reproduced from Dwiwedi et al. [18].*

Boyce and co-workers [22, 28] have conducted extensive studies on the material behaviour of PC over a wide range of strain rates in both compression and tension. Several experimental methods and instruments were employed for this purpose, including universal testing machines, the SHPB and the SHTB, and dynamic mechanical analysis (DMA).

Mulliken and Boyce [28] quoted earlier work in the literature when they stated that PC, and other engineering plastics, have significant rate dependency of the material yield behaviour. Beyond a transition threshold that is determined by both temperature and strain rate, the polymer is more sensitive to strain rate. In uniaxial compression tests, the significant strain rate dependency of the PC material was obvious, Figure 4.6, and the yield data indicated that the transition is centred around a strain rate of approximately 150 s^{-1}.

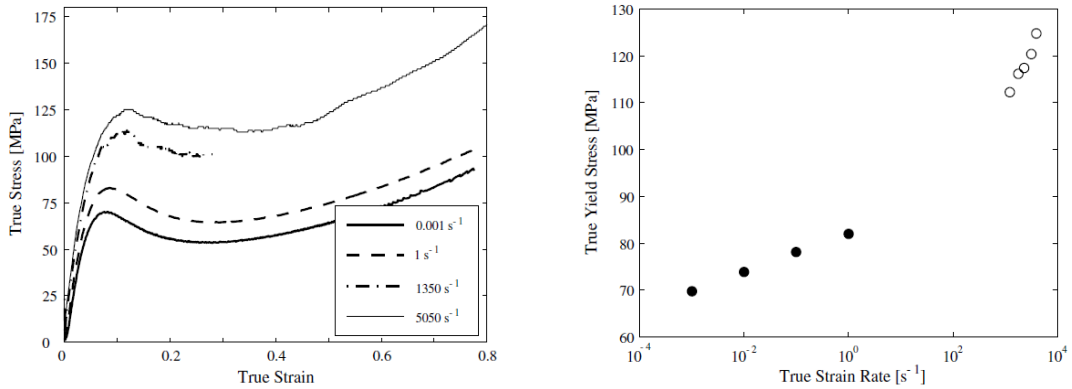

Figure 4.6 *True stress–true strain behaviour of polycarbonate in uniaxial compression at different strain rates (left), and true yield stress as a function of true strain rate (right). Reproduced with permission from Mulliken and Boyce [28].*

Mulliken and Boyce [28] also proposed a constitutive model for prediction of the deformation of amorphous polymers, including PC. The observed strain rate transition was consistent with the model predictions. The work by Mulliken and Boyce was supplemented by Sarva and Boyce [22], who conducted tensile testing of PC, and also finite element simulations. In this work, Sarva and Boyce also presented data on the necking behaviour of PC under high rate tension testing.

Siviour et al. [24] investigated the compressive stress–strain behaviour of PC at strain rates from 10^{-4} to 10^{4} s^{-1} at room temperature, and at temperatures from -50 to 150°C at 10^{3} s^{-1}. The testing was conducted with a universal testing machine and a SHPB. As can be seen in Figure 4.7, there were two distinct regions in the data at room temperature. High strain rates gave a much higher yield stress compared to quasi-static strain rates. Furthermore, the yield stress was strongly dependent on the temperature at high strain rates, and a higher yield stress was obtained at low temperatures, Figure 4.8.

4.3 Strain rate dependency

The strain rate dependency of PC and the presence of a transition threshold can be explained by motions at the molecular level [28]. When the degree of freedom of the polymer chain becomes restricted at high strain rate and/or low temperature, the overall material deformation resistance of the material is altered. It has been suggested that there is correlation between the observed transition in material yield behaviour with the secondary β-transition temperature. The β-transition has been attributed to the restriction of main-chain phenyl group rotations, but it has been suggested that other intermolecular motions are also involved. In analyses conducted by DMA, Mulliken and Boyce [28] found that the loss modulus had peaks centred at -95°C and

150°C, Figure 4.9, which correspond to the β- and α-transitions[5], respectively. Mulliken and Boyce also found a shift in the elastic modulus with increasing strain rate, Figure 4.9, which would also suggest there is a shift in the β-transition, and also the α-transition, towards higher temperatures.

Siviour et al. [24] also employed DMA to explain the transition threshold, or the bi-linearity as they refer to it, which was observed in their mechanical test results, Figure 4.7. The dependence of the yield stress on both strain rate and temperature was linked to molecular relaxations in the PC. Previous researchers had also observed that the yield stress of PC is bi-linearly dependent on the logarithm of the strain rate. The data presented by Siviour et al. showed that the bi-linearity is due to the shift of low order transitions (most notably the β-transition) in the materials, so that they occur at temperatures above room temperature at the higher strain rates. In other words, the increased yield strength at high strain rates is due to the β-transition being shifted to above room temperature at these strain rates. At a strain rate of 5500 s^{-1}, the upper end of the β-transition temperature was calculated to be approximately 40°C (compared to approximately -50°C at quasi-static strain rates). This was equivalent to the transition temperature for the bi-linear behaviour that was observed in compression, Figure 4.8.

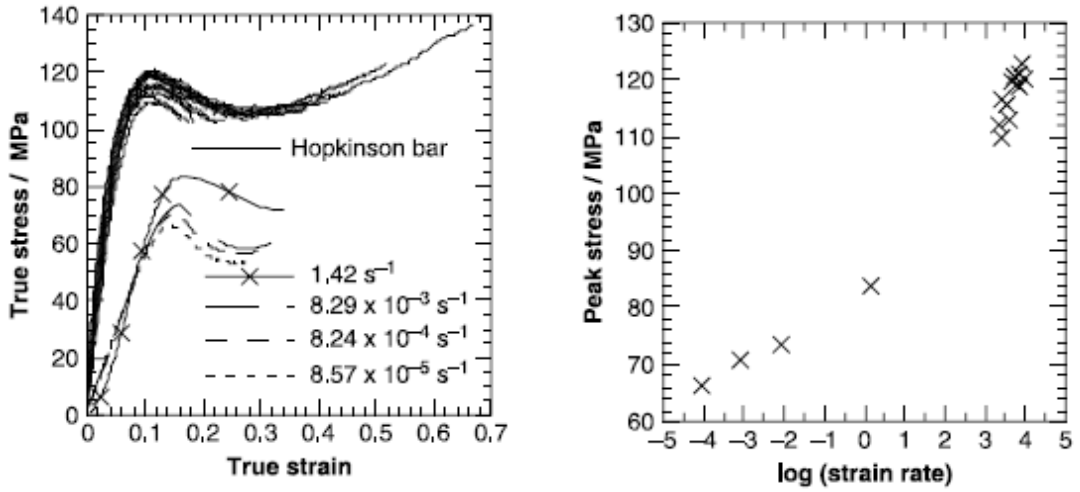

Figure 4.7 Room temperature compression stress–strain curves for polycarbonate, with the strain rates ranging from 2240 to 10280 s^{-1} for the split Hopkinson pressure bar (left), and a plot of peak stress against strain rate, showing the two distinct regions in the data (right). Reproduced with permission from Siviour et al. [24].

[5] The α-transition, or the α-relaxation temperature (T_α), is the same as the glass transition temperature (T_g).

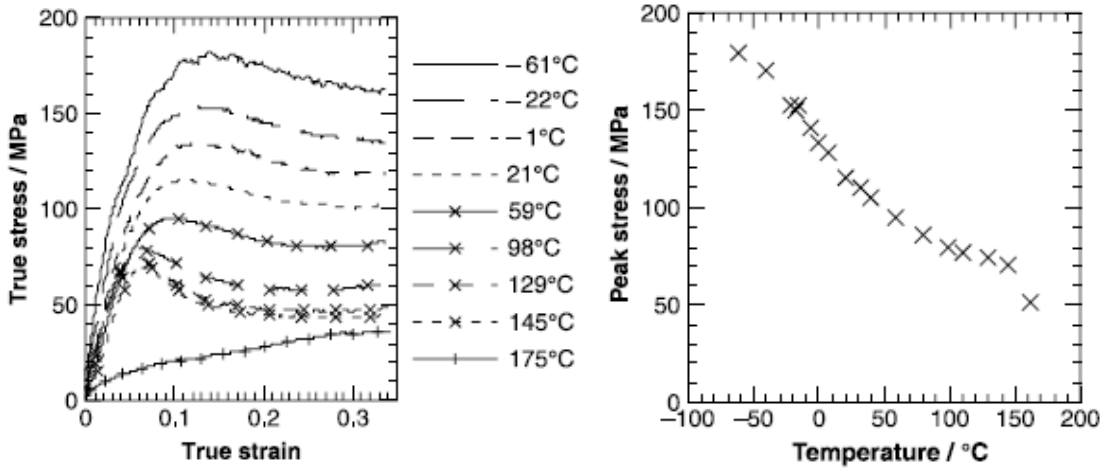

Figure 4.8 *Stress–strain curves for specimens of polycarbonate over a range of temperatures (left), and a plot of peak stress against temperature (right). The data sets were obtained using the split Hopkinson pressure bar at a strain rate of 5500±500 s^{-1}. Reproduced with permission from Siviour et al. [24].*

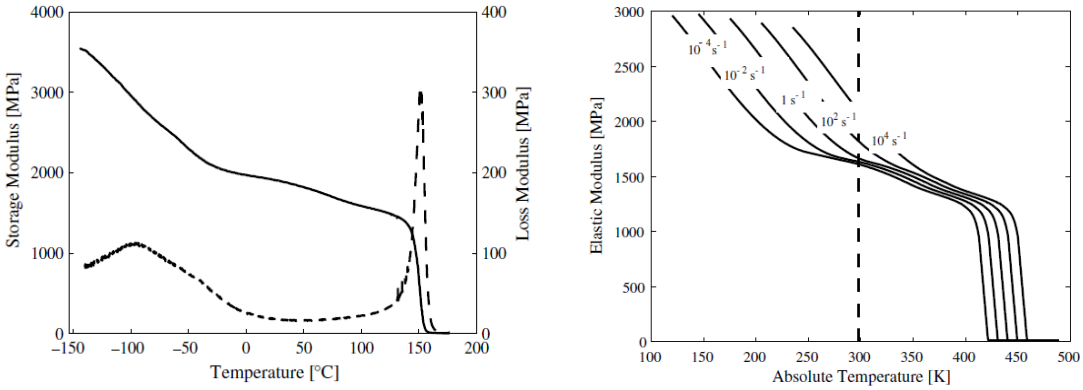

Figure 4.9 *Dynamic mechanical analysis of polycarbonate at a strain rate of 0.0032 s^{-1} (the solid line is the storage modulus and the dashed line is the loss modulus) (left), and model predictions of the elastic modulus at different strain rates (right). Reproduced with permission from Mulliken and Boyce [28].*

5 Ballistic impact on polycarbonate

5.1 Thin plates

5.1.1 Failure mechanisms

Wright et al. [29] described the ballistic failure mechanisms of polycarbonate in great detail and only an overview will be given here. Five penetration mechanisms were identified in PC plates with thickness 2, 5 and 12 mm: dishing, petalling (i.e. radial cracks that are propagating from the point of perforation), deep penetration, cone cracking and plugging. For spherical projectiles, as shown in Figure 5.1, the mode of failure was always petalling, and it was preceded by dishing for thin plates and deep penetration for thick plates. For cylindrical projectiles, as shown in Figure 5.2, cone cracking was the mode of failure for thin and intermediate plates, while it was plugging for thick plates. The plugging failure of the thick plates was preceded by deep penetration. Hence, it was apparent that the penetration mechanism was depended both on the projectile shape and the plate thickness. (The actual test data from Wright et al. [29] are described in Section 5.1.2.)

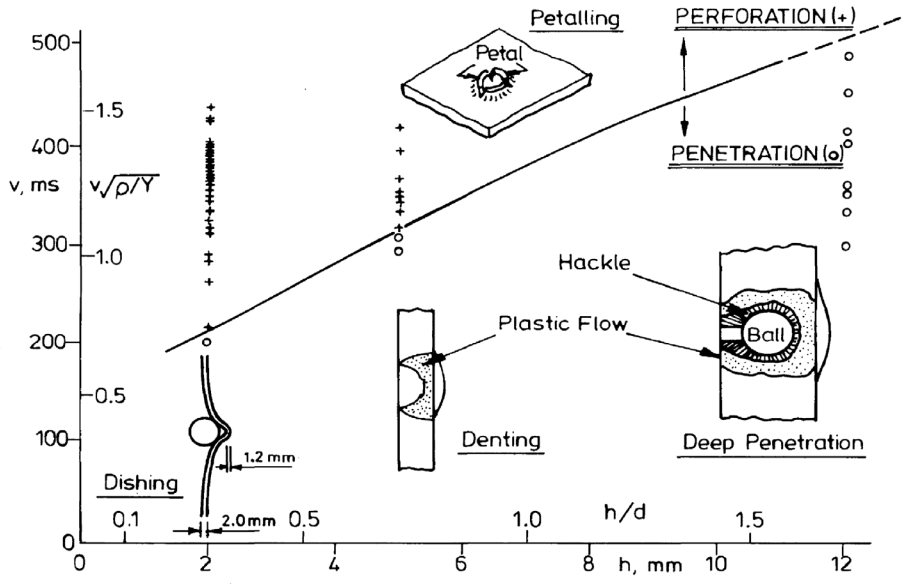

Figure 5.1 Failure mechanisms for ballistic impact on polycarbonate by spherical projectiles. Reproduced with permission from Wright et al. [29].[6]

[6] The non-dimensional group $v(\rho/Y)^{½}$ and h/d , where v is the impact velocity, ρ is the PC density, Y is the quasi-static compressive yield stress, h is the PC thickness and d is the projectile diameter, are also given. Inertia effects dominate the response when $v(\rho/Y)^{½} \gg 1$, while the response is quasi-static when $v(\rho/Y)^{½} \ll 1$.

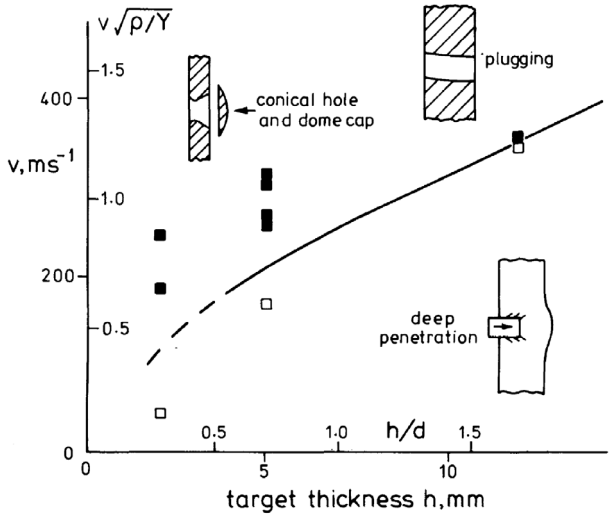

Figure 5.2 *Failure mechanisms for ballistic impact on polycarbonate by flat-ended cylindrical projectiles. Reproduced with permission from Wright et al. [29].*

Woodward and Cimpoeru [30] discussed the failure mechanisms found upon projectile impact on aluminium laminates. These findings also help explain how PC plates respond under projectile impact. Shear plugging was generally observed for thick targets, particularly for flat-ended projectiles Figure 5.3. Discing failure can also be observed in thick targets. It is a result of in-plane shear cracks formed as a consequence of in-plane shear stresses induced by bending combined with material weaknesses in the plane of the plate. Thinner plates favour more extensive dishing of the target, which involves energy absorption by stretching and bending. The stretching of the sheet can lead to ejection of a plug due to tensile failures at the edges (or the plug is folded away attached to a petal), or to necking and tearing in the form of a star pattern from the centre of the impact.

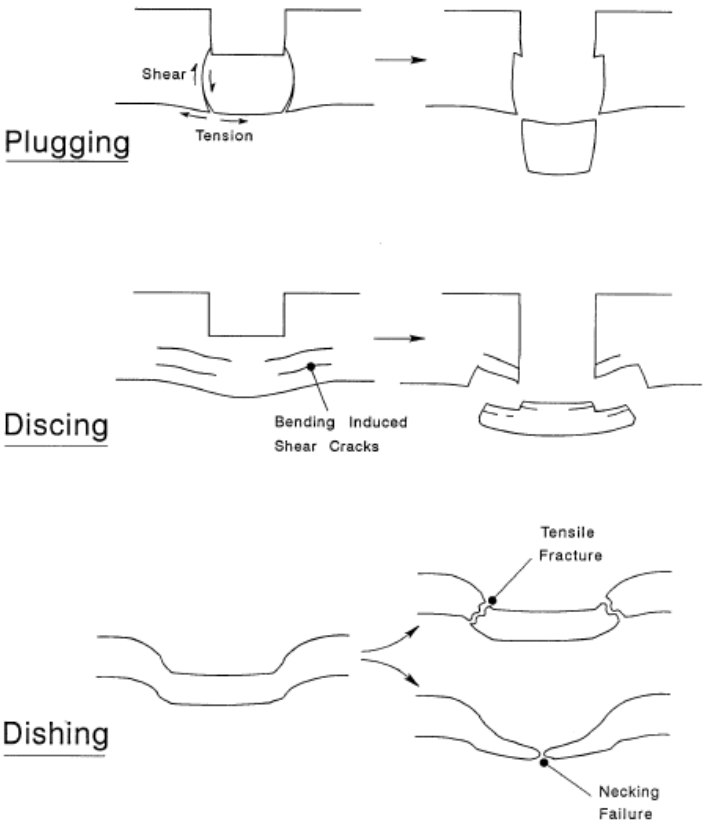

Figure 5.3 *Typical perforation mechanisms in homogeneous plates impacted by flat-ended projectiles. Shear plugging (top) and discing (middle) are generally observed for thick targets, and dishing (bottom) for thinner targets. Reproduced with permission from Woodward and Cimpoeru [30].*

A simple approach to quantitative modelling was also presented by Woodward and Cimpoeru [30]. Here, the perforation process was treated as one of indentation on the impact side followed by plug shearing for thick plates or by dishing for thinner plates. The model gave good estimates of the ballistic limit for both flat-ended and conical-tip projectiles. One finding was that dishing is favourable for plates of thickness less than one half of the projectile diameter. This agreed well with the experimental results, where thin plates failed by dishing and thick plates (> 1.17 projectile diameter thickness) failed by plugging.

The model was also able to provide reasonable predictions of the ballistic limit of PC targets impacted by conical-tip projectiles from the work of Radin and Goldsmith [31]. Thin targets were assumed to fail by a dishing mechanism whereas intermediate thickness targets (0.5 to 1.17 projectile diameter thickness) were assumed to fail by ductile hole formation.

5.1.2 Ballistic test data

The amount of information in the open literature about ballistic performance of thin PC plates is relatively scarce, but some papers present data on V_{50} ballistic limits. For example, the ballistic properties of several polymer materials, including PC, were summarised by Henry [3]. Henry provided results from V_{50} ballistic limit testing where PC of several different thicknesses was impacted by fragment simulating projectiles (FSPs). These results are summarised in Table 5.1.

Table 5.1 V_{50} ballistic limit of polycarbonate using fragment simulating projectiles (FSPs), as summarised by Henry [3].

PC thickness (mm)	FSP diameter (mm)	FSP mass (g)	V_{50} (m/s)
0.75	3.81	0.38	100-146
	5.59	1.1	--
	7.62	2.85	52-87
1.00	3.81	0.38	109-175
	5.59	1.1	86-116
	7.62	2.85	78-106
2.03	3.81	0.38	273
	5.59	1.1	190-195
	7.62	2.85	162
7.6[7]	5.59	1.1	299

Henry [3] also measured the masses of the plugs ejected when PC was penetrated by FSPs and 0.30 cal Ball projectiles, Table 5.2. Ejected material from an overmatching ballistic impact can also be termed as spall. Spall is an important consideration for transparent armour as its mass, velocity and form can present an ocular hazard to vehicle occupants, particularly if their eyes are in close proximity. One of the findings of Henry, was that there was little difference between the character of the ejected spall between different types and commercial brands of PC.

Henry reported that when a ductile material like PC is impacted by a flat-ended projectile, such as an FSP, a plug of approximately the diameter of the projectile is ejected by a process termed as ductile shear plugging. (Other failure mechanisms are possible, depending on PC thickness, projectile diameter and nose shape [30].) The plugging reported by Henry was not significantly

[7] Converted from an areal density of 9.15 kg/m^2 and a density of PC of 1200 kg/m^3.

affected by the presence of hard surface coatings on the PC. It was found that coatings with a thickness lower than 0.25 mm or so, did not alter the ballistic properties for the data reported in Table 5.2 (PC thickness is 3.2 mm or above). However, the ductile failure can change to brittle failure if the hard coating becomes too thick. On the other hand, for impacts by pointed 0.30 cal Ball projectiles, PC failure was by a 'closed hole' mechanism, which resulted in no ejected spall or mass loss, i.e. ductile hole formation.

Table 5.2 Spallation of polycarbonate from projectile impact, as summarised by Henry [3].

Material	Thickness (mm)	Projectile	Impact velocity (m/s)	Mass loss (g)	Spall description
PC	6.4	1.1 g FSP	304-334	0.36-0.46	Punched plug
Coated PC	3.2	1.1 g FSP	364	0.17	Punched plug
Coated PC	6.4	1.1 g FSP	316	0.46	Punched plug
PC	6.4	0.30 Ball	755-769	0.22-0.25	--
Coated PC	3.2	0.30 Ball	767	0.10	--
Coated PC	6.4	0.30 Ball	763	0.25	--

Hsieh et al. [32] also conducted impact experiments on monolithic PC of different thicknesses using 1.1 g FSPs. The results are shown in Figure 5.4. The V_{50} ballistic values that can be estimated from the figure are: ~110 m/s for ~0.8 mm PC, ~160 m/s for ~1.6 mm PC, ~210 m/s for ~3 mm PC, ~250 m/s for ~5.4 mm PC, ~350 m/s for ~9.2 mm PC, and ~400 m/s for ~13 mm PC. These results fall well in line with the results obtained by Henry [3] for the same 1.1 g FSP projectile. In addition, a layered structure of 3 mm PC, 12 mm PC and 3 mm PC, gave a V_{50} of 618 m/s and failure by localised plugging.

Impact experiments were also conducted on monolithic PMMA and different layered structures of PC, PMMA and glass. One finding was that monolithic PMMA gave higher V_{50} compared to monolithic PC, Figure 5.4.

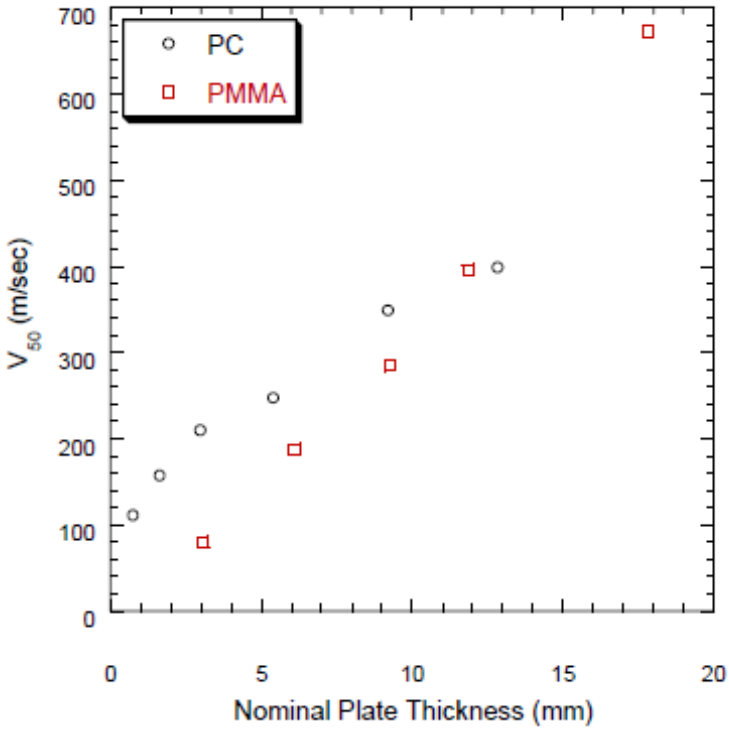

Figure 5.4 *V_{50} ballistic limit of polycarbonate and polymethylmetacrylate impacted by 1.1 g fragment simulating projectile. Reproduced from Hsieh et al. [32].*

Wright et al. [29] investigated the deformation and fracture mechanisms of PC plates during ballistic impact (as described in Section 5.1.1). The ballistic impact experiments were conducted on PC with thickness 2, 5 and 12 mm, and diameter 104 mm. Two types of projectiles were used: 7 mm diameter steel ball bearings of mass 1.4 g, and flat-ended silver steel cylinders with diameter 7 mm, length 9 mm and mass 2.8 g. Most of the tests were conducted with the steel ball bearings.

Non-perforating and perforating data for the two projectiles were presented. The V_{50} ballistic values were not actually calculated by Wright et al., but the data presented in Figure 5.1 and Figure 5.2 allow its approximate determination. For the spherical projectile, a V_{50} of ~210 m/s for 2 mm PC, ~320 m/s for the 5 mm PC, and ~500 m/s or above for the 12 mm PC, was estimated. For the cylindrical projectile, the V_{50} values were ~110 m/s for 2 mm PC, ~220 m/s for 5 mm PC, and ~350 m/s for 12 mm PC.

Tests with larger calibre projectiles have also been conducted. Radin and Goldsmith [31] impacted PC with two types of cylindrical 12.57 mm diameter steel projectiles with hardness R_C 56-59. The projectiles had either flat-ended (blunt) or 60° conical tips, with masses of 35 g and 29 g, respectively. The projectiles did not deform during the test.

Results from the ballistic testing are shown in Table 5.3. As can be seen in the table, for the thin PC plates the V_{50} ballistic limit is lower for the conical projectile, as would be expected. The conical projectile formed petals with dishing, at and just above the ballistic limit of the PC, Figure 5.5. Post-impact examination revealed that petalling was the main failure mechanism. The final hole shape in the PC exhibited a smaller diameter than the projectile, demonstrating some elastic recovery of the polymer. At similar impact velocities, the flat-ended projectile failed by plugging, producing a circular plug.

Table 5.3 *V_{50} ballistic limit of Lexan polycarbonate impacted by 12.57 mm diameter steel projectiles with two different nose shapes [31].*

PC thickness (mm)	V_{50} (m/s)	
	Flat-ended (mass 35 g)	60° conical (mass 29 g)
3.2	65.0	62.8
4.8	92.4	82.0
5.7	99.8	93.3
11.7	147	161.6

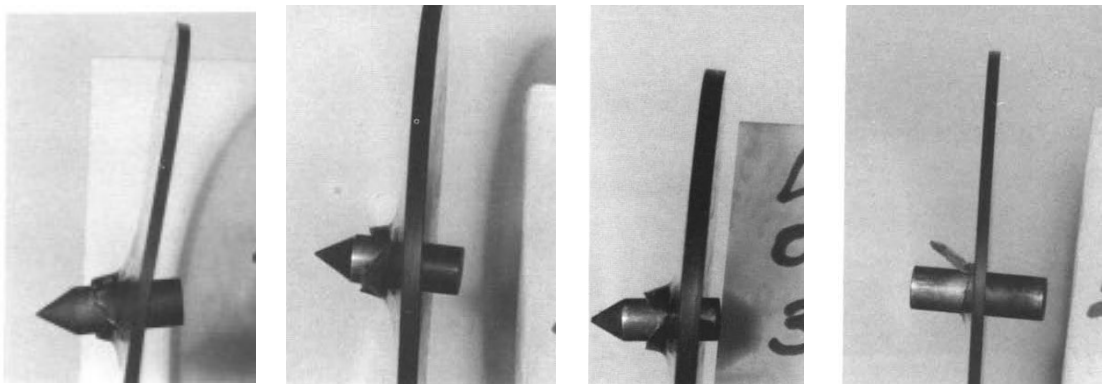

Conical, 3.2 mm PC, 62.9 m/s | Conical, 4.8 mm PC, 82.1 m/s | Conical, 6.35 mm PC, 93.9 m/s | Flat-ended, 3.2 mm PC, 65.0 m/s

Figure 5.5 *Polycarbonate plates perforated by 12.57 mm diameter conical and flat-ended projectiles at different impact velocities. Reproduced with permission from Radin and Goldsmith [31].*

The effect of different nose shapes of large calibre projectiles impacting on thin PC plates was also studied by Husain et al. [21]. Hardened steel projectiles with truncated conical or flat-ended nose shapes with a mass of 25.8 g and a diameter of 12.8 mm impacted plates with a thickness of 2.66 mm. The transition from non-perforation to perforation was ~80 m/s for flat-ended projectiles, and slightly lower at ~70 m/s for the truncated conical projectile. Similar studies were conducted by Landi et al. [33], who also found that the nose shape of even larger projectiles had an effect. Impact experiments with projectiles with three different nose shapes, all with diameter 20 mm and mass 100 g, on 4 mm PC were conducted. A flat-ended nose shape resulted in a V_{50} ballistic limit of 78 m/s, while truncated and prismatic nose shapes had slightly lower V_{50} values.

Shah and Abakr [17] investigated the effect of the distance from the support on the penetration mechanism of clamped PC. A 1.91 mm thick circular PC plate of 115 mm diameter was impacted by a 6.98 mm diameter spherical steel projectile. The impact velocity of 138 m/s was below the perforation limit of the plate, i.e. the impact velocity was below the V_{50} ballistic limit. Similar work was conducted by Shah [34]. Here, PC of thickness 1.5 mm was impacted by a 6.32 mm spherical steel projectile at an impact velocity of ~120 m/s. There was no focus on actually measuring the V_{50}, but rather on evaluation of the indents. Figure 5.6 shows an example of a dishing failure mechanism, as would be expected with this PC thickness and projectile diameter. Perforations were mainly discarded in this study, but the fact that most shots were stopped, while some perforated, indicates that the V_{50} was relatively close to the impact velocity of 120 m/s. However, both studies showed that the clamped edge had some effect, giving deeper dents closer to the edges of the plates than at their centre.

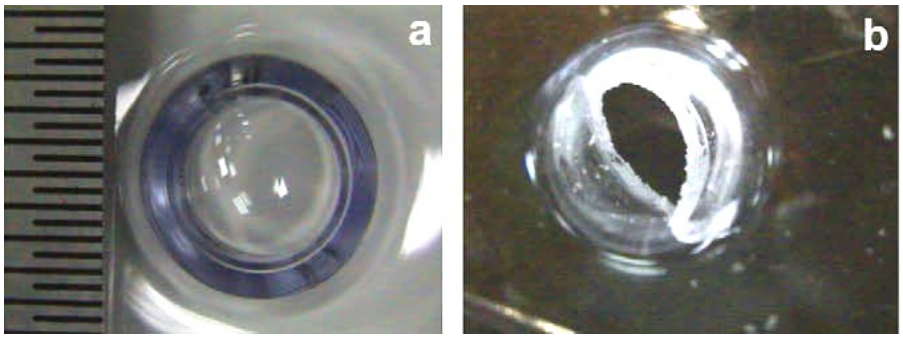

Figure 5.6 *Pictures of non-perforating (a) and perforating (b) impacts on 1.5 mm thickness polycarbonate impacted by 6.32 mm spherical steel projectiles. Reproduced with permission from Shah [34].*

The mechanisms that lead to brittle failure at low temperatures of glass/PC laminate constructions that were bonded with polyurethane were investigated by Walley et al. [35]. It had previously been observed in service that when laminates are impacted at low temperatures

(around -7°C or less), then the PC can fail with the ejection of a disc of material that is several centimetres in diameter, i.e. a discing failure mechanism. Steel sphere projectiles were fired at various target geometries at temperatures down to -8°C in a systematic study which included an investigation of the effect of double impacts. Examples of the results from laminate testing are shown in Figure 5.7.

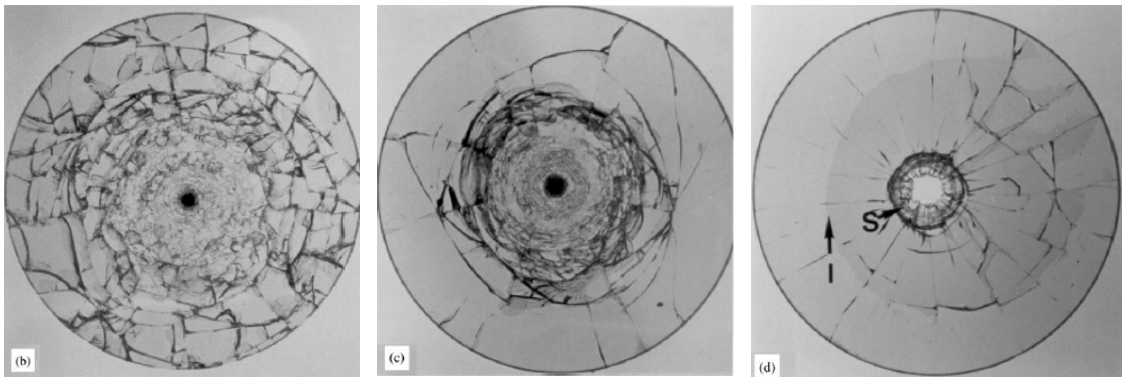

20°C -28.5°C -36°C

Figure 5.7 *Glass/polyurethane/polycarbonate laminate discs after impact with a 6 mm diameter steel sphere at 35 m/s. Material thickness was 3 mm/1 mm/3 mm. As the temperature is reduced, the amount of cracking in the glass is also reduced due to the increased rigidity of the polymer backing. Perforation occurred in the coldest specimen. Reproduced with permission from Walley et al. [35].*

For the glass/PU/PC laminates it was observed that spall formation took around ten times longer than a simple shock-wave overlap mechanism would imply. An elastic wave analysis for the glass was therefore employed. The main conclusion was that the Rayleigh surface wave in the glass will be reinforced by tensile elastic waves reflected from the various boundaries within the laminate, and that it will reinforce at distinct radii from the point of impact. This leads to bands of intense fracture which produce surface flaws on the PC but are able to penetrate the interlayer. Bending of the laminate causes cracks to initiate from these surface flaws if the temperature is low enough. The cracks then propagate in a ring around the impact point leading to detachment of a spall fragment or disc that was roughly circular in shape, Figure 5.8.

Neat PC targets were also impacted. One observation was that when 2 to 3 mm thick PC was impacted by a 4 mm spherical projectile at 310 to 340 m/s at room temperature, then the resulting perforation holes were smaller than the sphere diameter. This indicates that viscoelastic recovery of the polymer had taken place. This effect was not observed to the same extent at lower temperatures. Discing was not observed in the neat PC, however, the application of a PU-coating on the PC lead to a change in the failure mechanism at lower temperatures, resulting in the detachment of a disc of the polymer around 20 mm in diameter, Figure 5.8.

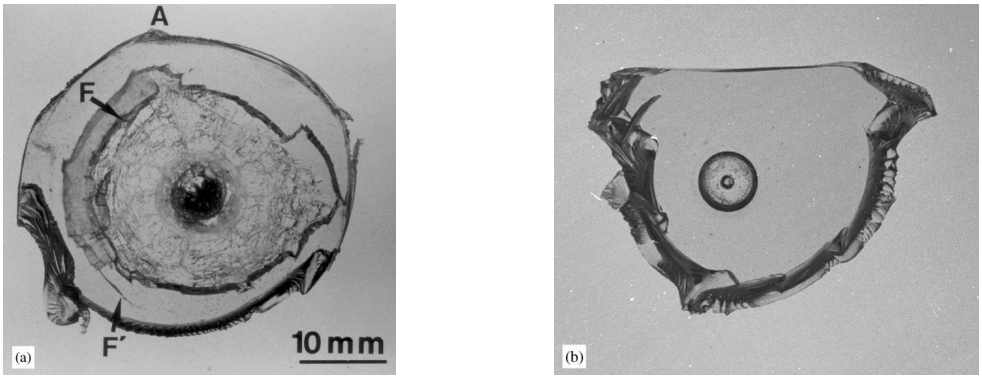

Glass/PU/PC laminate PU-coated PC

Figure 5.8 Typical spall fragment or disc formed during testing of the glass/polyurethane/polycarbonate laminate (left), and ejected spall fragment or disc from polyurethane-coated polycarbonate material impacted at 350 m/s and -30°C (right). Reproduced with permission from Walley et al. [35].

5.2 Thick plates

Ballistic impact on thicker PC plates has also been reported. For example, Dorogoy et al. [36] conducted ballistic testing of 50 mm thick PC plates with a 7.62 mm armour piercing projectile at various angles of inclination, including ricochet angles. Numerical modelling agreed well with the experimental projectile penetration paths.

Rosenberg and Kositski [37] have investigated the correlation between quasi-static indentation and ballistic penetration in PC. A clear correlation was observed between deep indentation tests with conical-nosed indenters and the penetration of 7.62 mm armour piercing projectiles. The resistance to penetration in both static and dynamic experiments was practically the same, which would imply that rate effects, i.e. strain rate sensitivity of flow stress, did not play a significant role in the penetration of PC. Hence, quasi-static mechanical properties with care may potentially be used as inexpensive ranking tools for evaluating PC materials and processing conditions.

Another use of thick plates where the PC is impacted by projectiles, is as a backing material in depth of penetration (DOP) tests [38, 39]. Compared to metals, which are the materials more commonly used in such tests, the strength and impedance of PC is much closer to that of the fibre composites commonly used as backing in ceramic armours, and the PC is also transparent, which facilitates efficient measurement of the penetration depth.

6 Ageing behaviour of polycarbonate

6.1 General

Polycarbonate has been subjected to ageing by ultraviolet light, temperature and humidity. The ageing has been reported to give two major effects. First, it alters the microstructure of the thermoplastic polymer, and also results in chain scission giving lower molecular weight polymer chains. Second, the change in microstructure has an effect on the material properties of the PC – one major change of ageing appears to be embrittlement of the material. The lower ductility has often been measured as a reduction in the elongation of failure in tensile tests. Several of the studies that have investigated the mechanical properties of PC after ageing will be discussed in more detail in Sections 6.2 and 6.3. However, no studies that correlate ageing and embrittlement with a possible change in ballistic performance have been identified.

Ram et al. [40] reported that the mechanical properties of PC after exposure to the atmosphere is affected by its sensitivity to UV radiation (photo-ageing) and to humidity, which causes hydrolysis and chemical breakdown. Thermal exposure also triggers various reactions leading to molecular chain degradation. According to Hill et al. [27]), physical ageing of thermoplastic polymers generally results in an increase in density, increase in tensile and flexural stress, increased elastic modulus, and higher stress drop after yield. At the same time, there is a decrease in impact strength, fracture energy, ultimate elongation, and creep rate. A transition from a ductile to a brittle fracture mode has also been shown to be a consequence of ageing.

The effect of ageing at a molecular level, apart from breakage of polymer chains, is that absorption of thermal energy and physical ageing is believed to give motion of the polymer chains, resulting in a higher packing density (decrease in free volume) without crystallisation. For PC, this is accompanied by changes in thermodynamic and material properties, such as an increase in the yield stress and the above mentioned embrittlement. The mechanisms for the embrittlement were discussed by Senden et al. [41], and was primarily explained in terms of intrinsic strain softening of the material (see Section 6.2).

6.2 Accelerated ageing

Sloan and Patterson [7] studied the effect of accelerated weathering of PC-based materials. Neat PC, and PC/silicate nanocomposite materials with a silicate loading of 2.0 and 3.5% by weight, were investigated. The PC was aged with an exposure cycle of 8 hours of UV radiation at 60°C followed by 4 hours of dark condensation at 40°C. Total exposure times up to 1000 hours were employed. The materials were characterized by UV/VIS spectroscopy and Fourier transform infrared (FTIR) spectroscopy.

The spectroscopic data showed clear evidence that the both filled and unfilled PC undergo a chain scission reaction where the carbonate structural linkages break when exposed to UV radiation similar to that found in natural sunlight. One suggested mechanism for the chain

scission is shown in the Figure 6.1. A significant amount of yellowing was observed in both the neat PC and PC/silicate nanocomposites. The PC nanocomposites demonstrated a much faster rate of yellowing than neat PC. Furthermore, a reasonable correlation was established between the carbonate scissions and the increase in material yellowing.

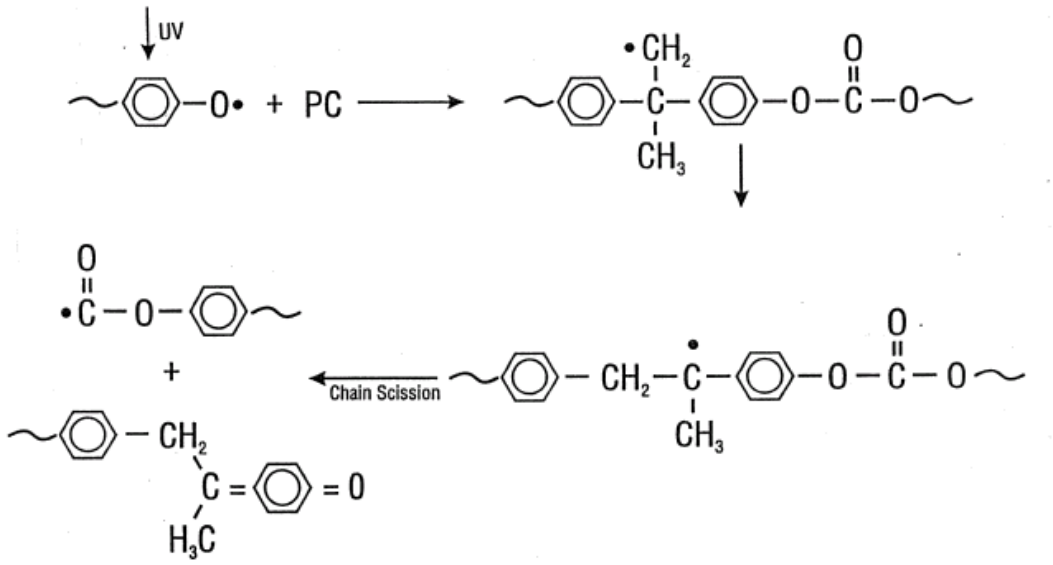

Figure 6.1 *Mechanism for chain scission upon exposure of polycarbonate to UV radiation, as suggested by Sloan and Patterson [7].*

Thermal ageing of PC was studied by Hill et al. [27]. Quasi-static tensile testing of 12.7 mm thickness sheets that were aged at 120°C in vacuum for 240 hours was conducted. The mechanical properties after ageing were significantly different from the as-extruded samples. Elongation of the as-extruded samples took place in a homogeneous manner for a few percent elongation (not quantified) up to yield, resulting in a yield strength of 68.0 MPa. The reduction in cross-sectional area was 46%. For the aged samples, an increase in tensile strength and a loss in ductility were observed, i.e. a yield strength of 76.9 MPa and reduction in cross-sectional area by only 10%.

Fracture toughness was also measured. For the fracture toughness, it was observed that the measured value was reduced from 3.23 to 2.63 MPa $m^{-½}$ as a result of the ageing. Both the aged and as-extruded specimens fractured in a brittle manner and no difference in the fracture morphology was observed by optical microscopy and scanning electron microscopy (SEM). However, the aged and as-extruded fracture surfaces in the tensile tests were markedly different.

The as-extruded fracture surface was relatively featureless, while the aged surface showed evidence of extensive crazing and multi-planar cracking.

Positron annihilation lifetime spectroscopy (PALS) was used to determine the change in PC free volume after the physical ageing. Ageing resulted in a reduction in free volume cavity size and concentration of cavities, which coincided with an increase in density. An increase in T_g was also observed after ageing. The effects of ageing on the molecular structure are thoroughly explained by Hill et al. [27], and the effect of thermal ageing on the free volume concentration is illustrated in Figure 6.2.

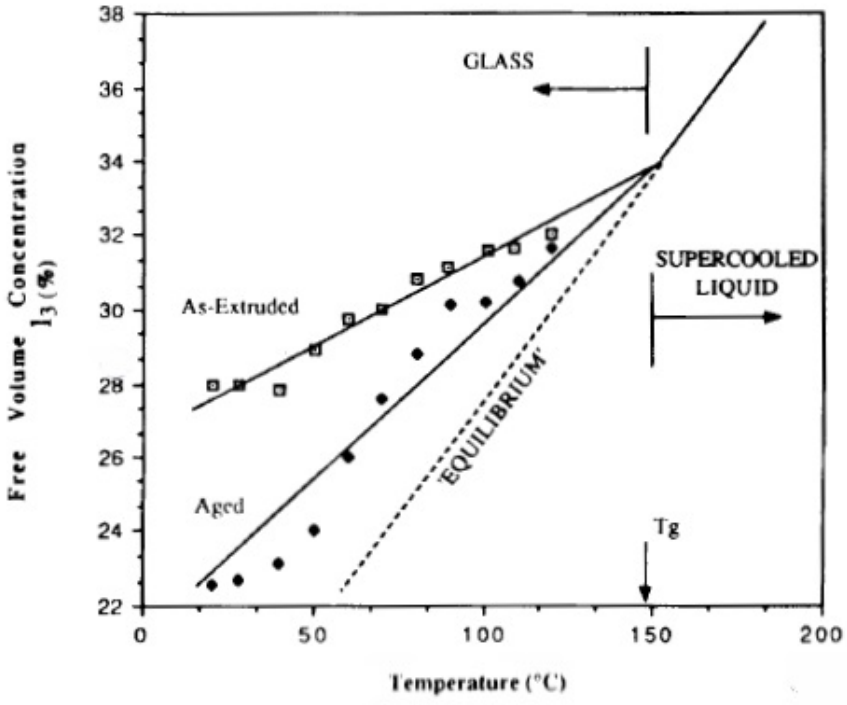

Figure 6.2 *Free volume concentration as a function of temperature below T_g for as-extruded polycarbonate and polycarbonate that has been aged at elevated temperature. Reproduced with permission from Hill et al. [27].*

The mechanisms for loss of ductility of PC upon ageing in dry air below the glass transition temperature was thoroughly discussed by Senden et al. [41] and the references therein. Annealing, or thermal ageing, will result in an increase in the yield stress. This increase in yield stress is accompanied by an increase in strain softening. This induces a more severe strain localization. Such softening will lead to the initiation of localised plastic deformation zones in stress concentrations. The higher the amount of strain softening, the more extreme this strain

localization will be, and the greater its triaxiality, reducing the effective strain to failure, with failure being accompanied by cavitation and craze initiation. Thermal ageing makes the material more vulnerable to stress concentrations such as notches from cutting, impurities, voids and microcavities. Hence, the fundamental cause for embrittlement due to thermal ageing of PC was explained to be caused by an increase in intrinsic strain softening.

Senden et al. [41] subjected three different molecular weight grades of Lexan PC to steam sterilization at 121°C. Tensile testing was conducted on injection moulded specimens at a strain rate of 10^{-3} s^{-1}, and size exclusion chromatography (SEC) was used to determine the molecular weights of the materials. All three grades of PC experienced a reduction in ductility with increasing ageing time. For PC materials with molecular weights above a critical level, reduced ductility was accompanied with an increase in yield stress. The same behaviour was not observed with lower molecular weight PC, since this material exhibited early brittle failure. For this low molecular weight material, the molecular weight was below a critical level where material properties may be affected[8].

The proposed mechanisms that contribute to PC embrittlement are hydrolysis, thermal ageing, and formation of microcavities. In this case, hydrolysis had no influence since the decrease in molecular weight was insignificant. However, it was found that thermal ageing played a major role since it decreased the ability of the material to delocalize strain, making the material much more vulnerable to stress concentrations. Microcavities that were observed to form during the steam sterilization then act as stress concentrations. Hence, the embrittlement of the PC was therefore an effect of, or an interplay between, thermal ageing and microcavity formation.

Sherman et al. [42] investigated the ageing of several grades of PC upon exposure to UV light. Commercial grades of Lexan PC were employed. The tensile properties of 3.4 mm thick samples (and thinner 0.2 to 0.3 mm samples) were investigated. The samples were exposed to UV light for up to 2500 hours, with water sprayed on for 10 minutes every hour. All samples were exposed on one side, and the temperature was maintained at 45°C. Tensile testing was conducted at a strain rate of 1.2×10^{-2} s^{-1}. Weathered surfaces and fracture surfaces were investigated by SEM, and molecular weights were measured by gel permeation chromatography (GPC).

Prior to exposure, the PC typically had a yield strength of around 62.8 MPa, an elastic modulus of 2.26 GPa, and an elongation at failure of around 115%. Of these mechanical properties, elongation at failure was the one that was most influenced by UV exposure. This is a good indication of the deterioration and loss of ductility of PC – faster crack growth in the material reduces sample elongation since it competes with the neck propagation rate.

Damage from UV/sunlight is primarily a surface effect. The exposed surface becomes more brittle than the interior, which will result in sites for crack initiation. These cracks can grow, merge, spread, and penetrate into the undamaged material below the surface layer, initiating failure at lower elongations and reducing toughness. The behaviour observed in the tensile tests

[8] For PC, the critical molecular weight is $M_w = 33800$ and $M_n = 14300$ [41].

correlated well with the changes in fracture morphology and molecular weight, as observed by SEM and GPC. The service lifetime of the samples, defined by a complete loss of ductility, was approximately 500-2000 hours of accelerated exposure, which corresponded to approximately one year outdoor exposure under Israeli climatic conditions.

de Melo et al. [12] investigated the influence of gamma radiation on the fracture toughness of PC sheets. Gamma radiation may not be relevant to many defence applications. However, gamma radiation has an effect at molecular level that is quite similar to physical ageing at elevated temperatures and humidity, and therefore the effect on the mechanical properties is of particular interest. Sheets of 4 mm thickness Lexan PC were used in the study. The fracture toughness tests were carried out using single edge-notched three point bend (SENB) specimens. Tensile testing at quasi-static rates, tests for determination of molecular weight, and FTIR spectroscopy for chemical analysis, were also carried out.

It was found that, as the gamma irradiation dose is increased, there is an increase in the chain scission in the carbonyl groups in the PC, and hence a decrease in the molecular weight. The mechanical properties of PC were therefore affected by gamma irradiation, and a gradual ductile-to-brittle transition was detected as the radiation dose increased, giving a reduction in the measured fracture toughness. This coincided with a slight decrease in tensile strength and elongation at failure. However, the differences in the mechanical properties were not dramatic, but investigation by microscopy confirmed the results of fracture toughness tests.

Hahn and Herzig [26] characterised naturally aged PC at strain rates of 0.001, 1.0, and 500 s^{-1}. Both tensile and compressive tests were conducted. The PC had been aged for 6-7 years, and one can only assume that the PC was subjected to elevated heat and humidity. The final application of the PC material was transparent armour.

Relatively similar results to other authors were found. The tensile strength was ~65 MPa at the lower strain rates, but increased to >80 MPa at the highest strain rate. The strain at failure was also reduced, reaching a minimum at a medium strain rate. The compression tests also showed a strong strain rate dependency, with higher strain rates giving higher strengths (>110 MPa). Nevertheless, both tensile and compression testing showed only minimal differences between non-aged and aged PC.

6.2.1 Prediction and modelling of ageing

Different models for predicting the lifetime of PC were evaluated by Kahlen et al. [43]. The models were based on the Arrhenius activation energy relationship, in which it is assumed that the degradation within a temperature range is controlled by a single thermally activated chemical process. One proposed method was based on the superposition of ageing curves obtained at different temperatures to a master curve by horizontal shifting along the time axes. The obtained shift factors were then analysed in terms of the Arrhenius relationship.

Kahlen et al. [43] employed tensile strain-to-break values as an indication of the degree of ageing of PC. It was found that the strain-to-break decreased both after exposure to hot air and

after immersion in hot water, and that the ageing was accelerated at higher temperatures. The hot water exposure resulted in lower activation energies, reflecting the sensitivity of PC to hot water.

The activation energies determined by the different models did not vary significantly, but very different expected lifetimes of PC were deduced. For example, based on residual strain-to-break requirements, the lifetime was in the range 17 to 204 years in air at 90°C and 5 to 58 years in water at 40°C. These results raised the question of the reasonability of the various models when applied to PC.

The principle of constructing master curves, using time-temperature superposition of test results obtained at different temperatures, was also discussed by Engels et al. [15]. This approach could be used to predict the long-term embrittlement upon ageing of PC. However, it was pointed out that care should be taken whenever using this approach, since the underlying assumption is that the degradation mechanism is the same at different temperatures, but this may not always be the case.

6.3 Natural weathering

Ram et al. [40] continued the study of Sherman et al. [42] with a focus on assessing the life expectancy of several grades of commercial Lexan PC. The different grades had different molecular weights and degrees of stabilization. Ageing was conducted by three different methods for periods up to 2.5 years: (i) natural weathering with the PC attached to exposure racks at 45° and facing towards the south; (ii) accelerated weathering in a chamber with exposure to UV radiation and water sprays for 10 minutes each hour (the same conditions as used by Sherman et al. [42]); and (iii) thermal ageing at up to 80°C in ovens with air circulation. In addition to tensile testing, Izod impact testing was also conducted.

Tensile stress-strain curves of the un-aged PC showed a short elastic region, yield at ~10% elongation, and ductile extension after necking without strain hardening until failure at ~110% elongation. The main effect of material deterioration during ageing exposure was seen as a reduction in the elongation, which relates to a loss of ductility of the PC. Examples of tensile elongation of the different ageing conditions are shown in Figure 6.3. The combination of heat and humidity seemed to be the critical causes for catastrophic embrittlement. Loss of optical clarity and chain scission, giving a reduction in the molecular weight, were also observed. However, the impact strength was less affected.

The correlation between natural and accelerated weathering was estimated to be approximately 6:1, that is 1500 hours (or two months) in the exposure chamber was equivalent to one year of natural ageing. A maximum lifetime of at least three years under the severe weather conditions was predicted for the best-performing grades of PC. These grades were of high molecular weight and contained stabilisers.

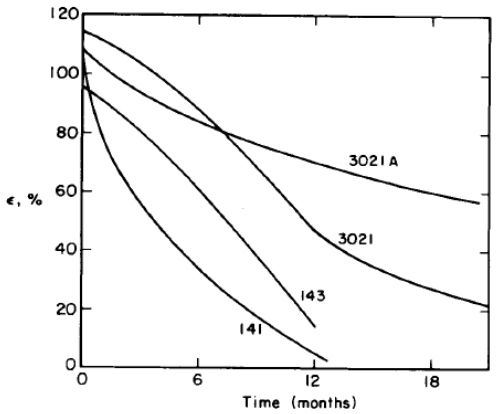

Natural weathering (outdoors in Israeli conditions)

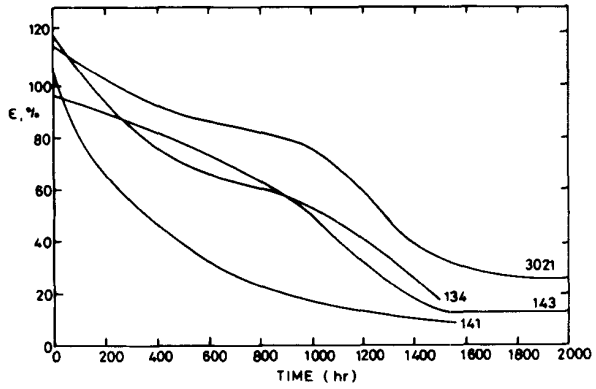

Accelerated weathering (UV radiation and spraying with water)

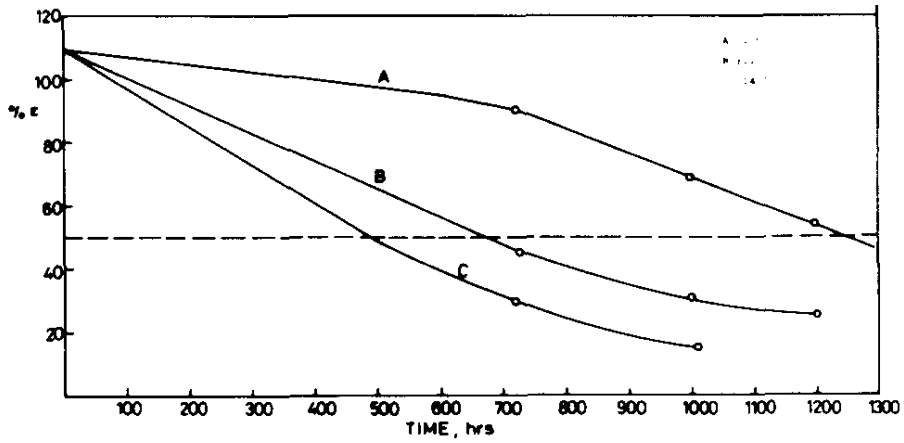

Thermal ageing

Figure 6.3 Tensile elongation of different grades of polycarbonate as the result of different ageing procedures. Reproduced with permission from Ram et al. [40].

7 Ageing of transparent armour

Ageing of transparent armour, which is constructed as a layered systems of different materials, is a somewhat more complex case than ageing of a single polycarbonate layer. The same effects seen in PC, as discussed above, may also be taking place in the PC laminate within an armour system, but the degradation of the adhesive interlayers may be equally, or even more, important. Furthermore, in a layered armour system, it is not only the mechanical properties of the materials that may be affected, but also the transparency of the armour, which is often affected by degradation of, or delamination between, the interlayers. Some possible causes for ageing damage in transparent armour are illustrated in Figure 7.1.

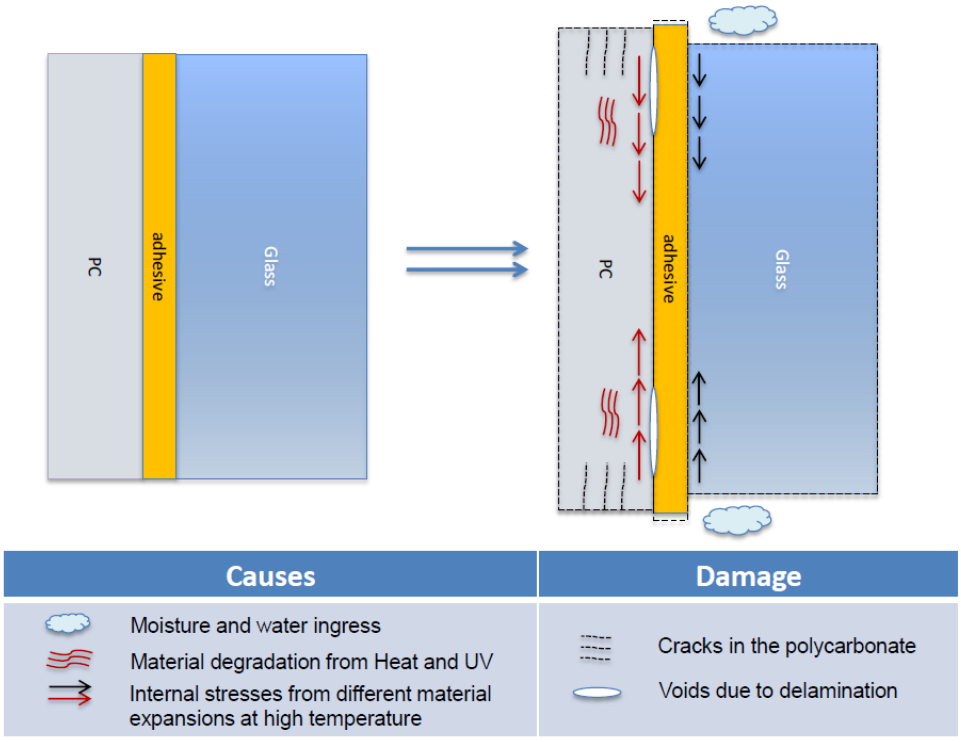

Figure 7.1 *Possible causes of ageing damage in transparent armour, as suggested by Yang et al. [2].*

The degradation of the PC and the interlayer is also likely to be dependent on many factors, such as the design of the vehicle, stresses from the transparent armour framing, possibly caused by poor fit-up to the vehicle hull, the in-service use of the vehicles and of course the exact materials used and production process for the transparent armour.

7.1 Polycarbonate layer

Yang et al. [2] conducted multi-hit ballistic testing on transparent armour that had been installed on vehicles for around 4-5 years. In service, the armour panels were exposed to hot and humid climates, and extreme UV. Different behaviour was observed for new and aged armour during the ballistic testing. For new armour, the PC layer underwent large deformations when absorbing the projectile impact. For shots that completely perforated the armour, there was also ductile behaviour with the bonding of the PC layer to the glass remaining intact, Figure 7.2. In armour that had been aged on vehicles, delamination was present and impacts resulted in cracking and ejection of significant fragments of the PC. Discoloration and severe delamination of the PC layer was also observed in these panels. The main conclusion was that ageing results in embrittlement and delamination of the PC layer and reduced ballistic protection.

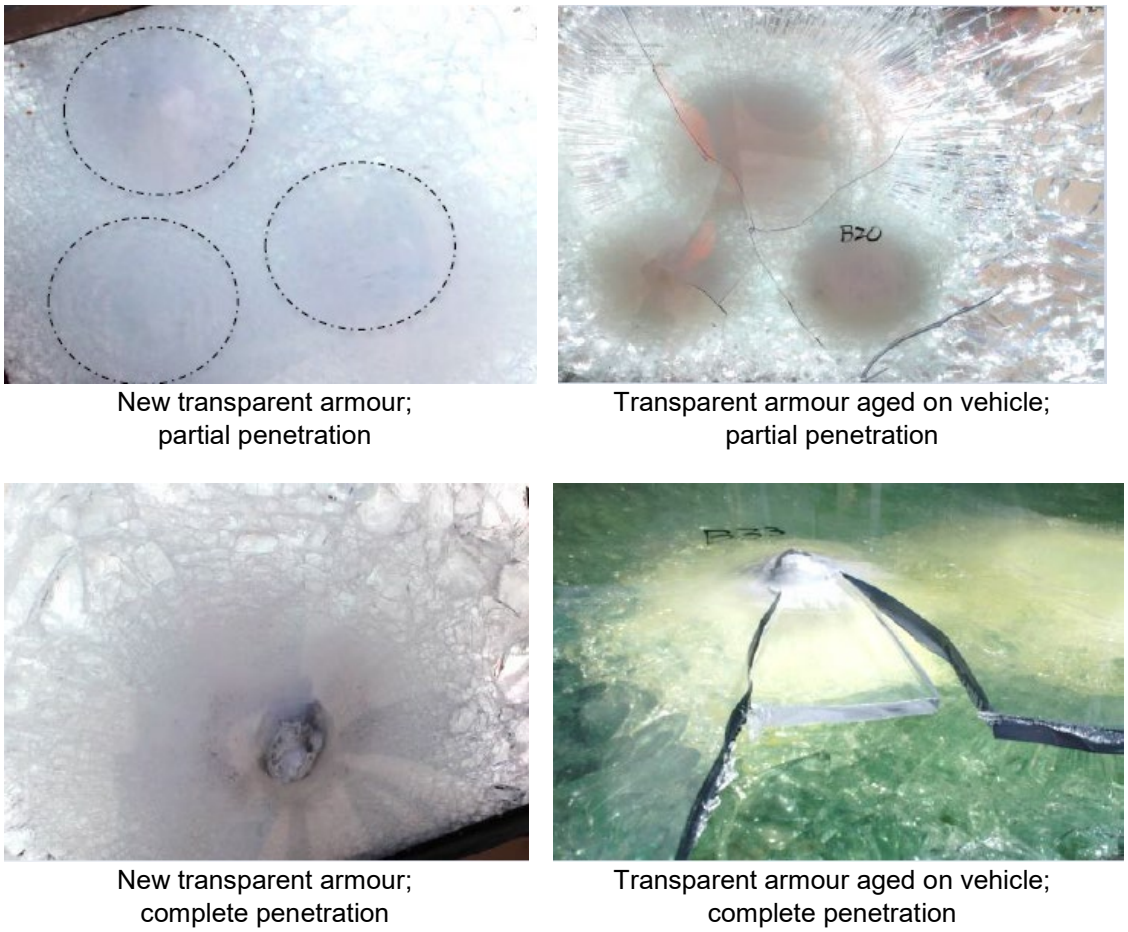

New transparent armour; partial penetration

Transparent armour aged on vehicle; partial penetration

New transparent armour; complete penetration

Transparent armour aged on vehicle; complete penetration

Figure 7.2 Pictures of tested transparent armour panels. Reproduced from Yang et al. [2].

The work of Yang et al. [2] was continued by Holmes et al. [44], who conducted natural ageing of transparent armour over a period of years in a tropical climate of high temperature, high humidity and extreme levels of UV exposure. So-called environmental monitoring units (EMU's) were employed during the ageing, such that the PC layer was exposed to temperatures and humidity of a vehicle cabin-like environment and the outside of the transparent armour to the external climatic conditions. The inside and outside temperatures were continuously monitored, and temperature discrepancies between the two surfaces were observed. The recorded data qualitatively described the real-word conditions that transparent armour may be exposed to and could be related to delaminations that were observed. The data collected provide indicative cycles for future climatic chamber testing.

Differences in material behaviour and ballistic properties between new and used transparent armour have also been observed by other authors. For example, PC in the pristine state and aged in-service was also tested by Welker et al. [45]. The PC was found to be relatively insensitive compared to the interlayer materials, and no significant changes in mechanical properties under dynamic loading could be detected. It is possible that the threshold for degradation had not been reached.

Similar observations were made by Balkova et al. [46]. They studied PC from degraded transparent armour that had been used in-service on vehicles for up to nine years. However, the tests revealed that the mechanical and thermal properties of the PC were unchanged when comparing to the pristine material. Hence, the PC itself was not degraded during use. Instead, the degradation of the armour was related to degradation of interlayers.

7.2 Interlayer

The adhesive interlayer between the different laminates is a critical part of transparent armour systems. Degradation of the adhesive interlayer can cause debonding between laminates, and also result in the armour becoming partially or fully opaque. This can give reduced visibility, reduced protective capability and significantly increased operating costs [47]. It is believed that the degradation of the armour system is governed by environmental factors, which can be exacerbated by the thermal mismatch between materials and therefore thermally induced strains.

Replacing degraded transparent armour on vehicles comes at a significant cost. This was recently demonstrated in an extensive report by Pint et al. [48]. The U.S. Marine Corps has approximately 16,000 tactical vehicles that require transparent armour. It was observed that a significant percentage of the vehicles have delaminations in critical areas of their windshields, particularly in the HMMWV[9] and MTVR[10] fleets. Extensive delamination was estimated to occur after an average of four to six years in service. It was estimated that it would cost approximately USD 272 million over ten years to immediately replace all delaminated windshields and restore full vehicle availability. As an example, a new LVSR[11] windshield

[9] High Mobility Multipurpose Wheeled Vehicle.
[10] Medium Tactical Vehicle Replacement.
[11] Logistics Vehicle System Replacement.

panel costs as much as about USD 7,200, although estimates showed that windshields could be repaired at a cost of USD 3,600.

Balkova et al. [46] reported that degradation of transparent armour had been observed on military vehicles used by several NATO countries, where a loss of transparency occurred after as little as three years in service. Typical behaviour was that the armour first became white along the edges, which then spread towards the centre. In the final stage, more white areas were formed, Figure 7.3. At first, the white appearance was fully transparent, but the armour gradually turned completely white and became almost opaque. The whole degradation process was very quick and occurred in a matter of weeks after the first signs of the white colouring occurring.

Carton [49] also observed the formation of a white phase in the interphase between PC and the bond film in a transparent armour from several fielded vehicles. In this particular type of transparent armour, chemical analyses showed that the white phase was caused by segregation of a UV stabilizer that was present in the PC or the bond film. This caused reduced transparency, reduced bond strength and delamination.

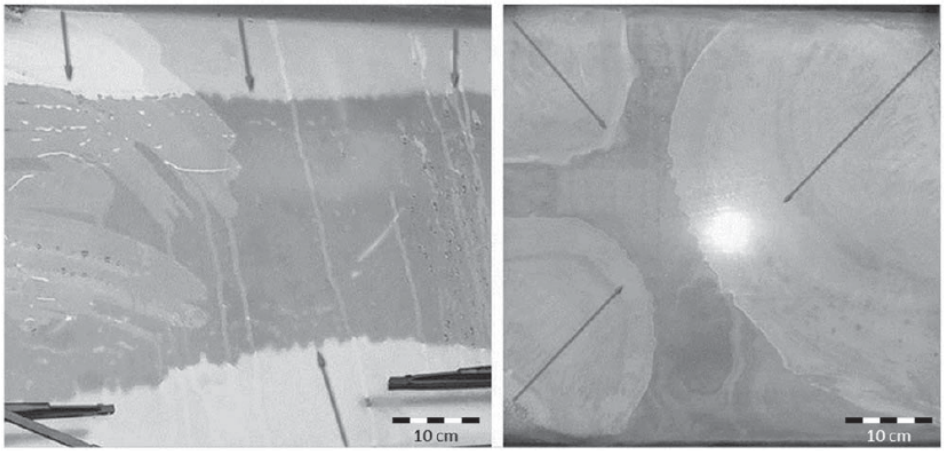

Figure 7.3 Pictures of transparent armour aged on vehicles. Reproduced with permission from Balkova et al. [46].

The transparent armour considered by Balkova et al. [46], consisted of four soda-lime-silica glass sheets bonded by a polyvinyl butyral (PVB) adhesive film and one PC sheet bonded by a polyurethane adhesive film. Thermoplastic polyurethanes (TPUs) are often preferred for adhesion to PC, rather than other polymers, since they do not contain plasticisers that are known to attack polymers such as PC [47]. The degradation of the transparent armour, because of a loss

of transparency, was nevertheless found to have been caused by changes in the PU adhesive. Delamination between the PC sheet and the PU adhesive, and the formation of a fine white powder on the PC surface, were observed. It was postulated that the main reason for the degradation was the thermal expansion mismatch between the different materials, i.e. the soda-lime-silica glass, the PU adhesive and the PC sheet. The PU adhesive is a semi-crystalline material with a molecular structure that is sensitive to temperature. In the temperature range that the vehicles operated, the polymer can recrystallize and, hence, change density, mechanical properties and appearance.

Furthermore, Balkova et al. [46] conducted both dynamic and static tension creep tests on smaller components at a range of temperatures. In these tests, it was found that 70°C was the critical temperature where the different thermal expansions of the PC and the PU adhesive started to have an effect. It was assumed that the degradation of the in-service armour in the vehicles then started in locations of high stress concentration at around this temperature.

Parker et al. [50] stated that the temperatures within the transparent armour windows are known to reach 70°C in field conditions. At such elevated temperatures PC readily undergoes hydrolysis where water molecules are able to break various bonds within the PC matrix. These broken bonds result in a degradation of the mechanical properties of the PC, i.e. embrittlement. Additionally, mobile molecular fragments are produced by this bond breaking that can diffuse and effect/interrupt bonding interfaces. This can in principle lead to delamination of the PC from the rest of the transparent armour.

Welker et al. [45] investigated the ageing behaviour of polymers used as interlayers in transparent armour. Such polymers were thought to be highly sensitive to heat, humidity and UV radiation. Two different variants of PVB and one TPU were thermally aged at 90°C and 30% relative humidity for up to 14 days, and the physical and chemical degradation was investigated by quasi-static tensile testing and Fourier transform infrared spectroscopy.

The ageing conditions had a significant effect on the properties of the interlayer materials. For both PVB variants, a significant increase in the elastic modulus and embrittlement was observed, the degradation was believed to be caused by a chemical or diffusion-based reduction of the plasticizer in the material. For the TPU, a significant decrease in the elastic modulus and softening was observed. Ageing of TPU was believed to occur through a mechanism of chemical reduction of ‘hard’ segments in the polymer chain. However, the mechanical behaviour changed very early after the start of thermal exposure and remained nearly constant for longer ageing periods, so for TPU used in laminates the softening may already be caused by the lamination process as initial conditioning and not actual ageing.

The bond strength of glass/TPU/PC samples that were cut from complete transparent armour were also tested by a quasi-static out-of-plane tensile test. It was found that the thermal ageing resulted in a weaker bond between the glass and the TPU. The failure was initially cohesive, i.e. failure within the TPU interlayer, but then shifted to adhesive failure between the glass and the TPU with prolonged exposure times. These investigations also showed that moisture diffusion from the PC surface to the interlayer is another potential environmental degradation mechanism.

The effect of the more realistic ageing condition of 60°C and 30% relative humidity was also investigated by Welker et al. [51]. They found that the adhesive interlayer was less affected at this condition, especially when diffusion was reduced by covering the samples to simulate a laminate with glass.

In further work, Welker et al. [52] investigated the effect of strain rate, temperature (-32, 20 and 44ºC) and hot/wet ageing of PC, PVB and TPU. A common observation for all three materials was that the material behaviour is strongly strain rate- and temperature-dependent. These effects were clearly more dominant here than the influence of natural and artificial ageing, the degree of natural ageing imparted not having a significant effect on the measured properties. Nevertheless, artificial ageing resulted in increased stiffness of PC under tensile loading. For the PVB material, artificial ageing gave a significant increase in stiffness particularly under compressive loading. No significant influence of artificial ageing of the TPU material was observed.

Rivers et al. [53] studied the influence of moisture and thermal cycling on delamination in glass/PC transparent armour. Transparent armours in service were exposed to temperature, moisture and UV light, which resulted in delaminations. According to Rivers et al., the exact delamination mechanisms were unknown, but believed to be: (i) interlayer thermal stresses; (ii) thermal cycling; (iii) moisture ingress; and (iv) chemical degradation, such as hydrolysis or photo-degradation of the polymer chains. Temperature and moisture seem to have had the most significant effect.

Small coupon specimens made of soda-lime-silica float glass and PC with an interlayer of aliphatic TPU were investigated. The specimens were subjected to hydrothermal and thermal ageing treatments, both in a water bath and in a dynamic mechanical analyser. Some ageing cycles successfully produced repeatable delaminations in the TPU interlayer, Figure 7.4. It was proposed that crystalline segments in the thermoplastic polymer were disrupted by moisture diffusion, the higher temperature then causing diffusion of the crystalline segments, which then subsequently re-crystallized at interfaces. This will lower the adhesive strength and result in delaminations.

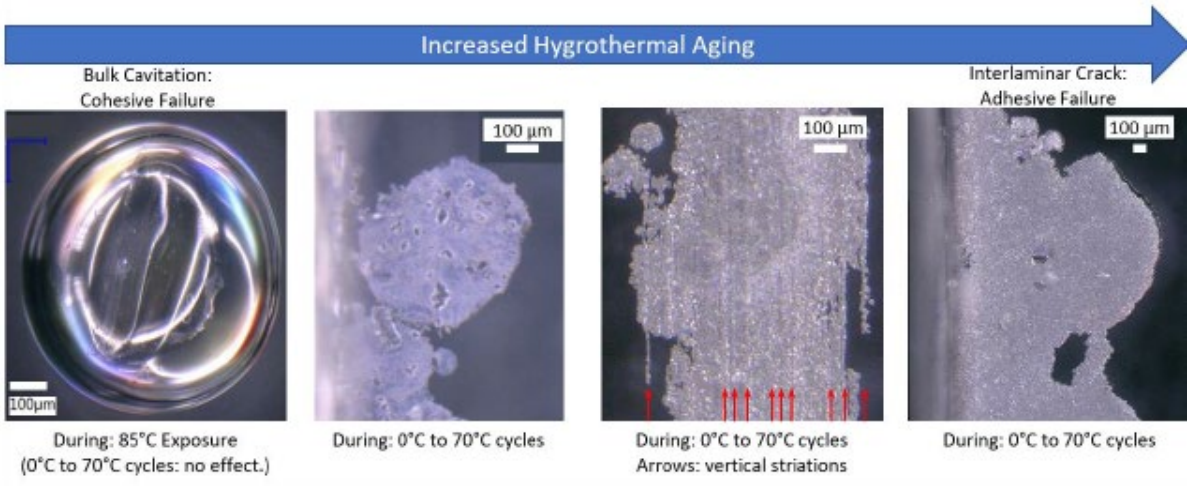

Figure 7.4 Delamination in glass/thermoplastic polyurethane/polycarbonate specimens. Reproduced with permission from Rivers et al. [53].

8 Summary

Transparent armour on military ground vehicles is a layered system of different transparent materials (most common materials are glass and polycarbonate (PC)). It is designed to provide protection against projectiles and fragments. These materials have very different physical properties, and behave very differently during ballistic impact and during their service life. Transparent armour is optimised with respect to ballistic performance, weight and cost.

PC is usually chosen as the backing layer, or spall layer, in transparent armour (and also as the stand-alone material in applications such as goggles and visors). It is primarily employed because its excellent in-plane and through-the-thickness ductility facilitate the formation of a ductile failure mechanism rather than a low-energy brittle failure mechanism. While the PC backing by itself does not play a major role in defeating the projectile, its other main role is to contain the eroded projectile and fragments, including glass debris.

The tensile deformation behaviour of PC is similar to that of many other polymers. It typically consists of a linear elastic and non-linear elastic deformation stage, a yield drop, initiation and propagation of a necked region, followed by strain hardening and failure. Typical material properties include a tensile strength of 66 MPa, a tensile modulus of 2.2 GPa, and a tensile elongation of 90-120%. Testing in compression typically gives slightly higher values for the compressive strength and the compressive modulus, the different material behaviour being explained by different molecular orientations between tension and compression.

The material properties of PC are strongly strain rate dependent, both in tension and compression, and there is always an increase in the yield stress with increasing strain rate. The rate dependence is linked to molecular relaxations in the material. In compression, it has been observed that there is a bi-linearity in the material behaviour, and that the strain rate effect on the apparent yield stress becomes more dramatic between quasi-static and high rate loading. Enhanced hardening has been reported to occur above a threshold of 10 to 100 s^{-1}. The properties of PC are also temperature-dependent.

PC is a ductile material and sheets that are impacted by different projectiles will fail by plastic deformation. Several penetration mechanisms have been identified, such as dishing, petalling (i.e. radial cracks that are propagating from the point of impact), discing (formation of a disc that is ejected), deep penetration, cone cracking and plugging. However, it is apparent that the penetration mechanism is dependent on both the projectile shape and the plate thickness. For example, thinner plates may favour more extensive dishing of the target, while thicker plates may favour plugging failures. There is often a combination of penetration mechanisms that occur during an impact process.

Although PC has some excellent properties that make it suitable for use in ballistic protection, it also has some major drawbacks. The material properties of the PC are known to degrade when exposed to ageing conditions, such as ultraviolet (UV) light, humidity and temperature. On a molecular level, ageing may result in chain scission, resulting in a lower molecular weight of

the polymer and in molecular motions, resulting in higher packing density without crystallisation. These effects will result in lower ductility and embrittlement of the material. For this reason, components that include PC may experience reduced ballistic performance after a period in service.

In transparent armour ageing, both the degradation of the PC and the adhesive interlayer may contribute to the failure of the armour to fulfil its purpose. The embrittlement of the PC may well be critical for the ballistic performance, while the degradation of the interlayer is critical to transparency.

Thermoplastic polyurethane (TPU) is often the preferred choice for bonding of glass/PC in transparent armour. However, there are several examples of degradation of the TPU interlayer that have caused delamination, including on vehicles in service, resulting in the armour becoming partially or fully opaque. It has been postulated that the main reason for the degradation is environmental factors, and it is believed that such degradation can be exacerbated by the thermal mismatch between different materials inducing thermal strains.

Ageing of PC results in the transparent armour having a lifetime that is much shorter than that of vehicles. The replacement costs of transparent armour for military ground vehicles is high, and the consequence of premature ageing is significantly increased operating costs.

List of terms and abbreviations

AlON	Aluminium oxynitride
DOP	Depth of penetration
DMA	Dynamic mechanical analysis
FSP	Fragment simulating projectile
FTIR	Fourier transform infrared
GPC	Gel permeation chromatography
HEI	High Explosive Incendiary
HMMWV	High Mobility Multipurpose Wheeled Vehicle
LVSR	Logistics Vehicle System Replacement
M-ATV	MRAP All-Terrain Vehicle
M_n	Number-average molecular weight
MRAP	Mine Resistant Ambush Protected
MTVR	Medium Tactical Vehicle Replacement
M_w	Weight-average molecular weight
PALS	Positron annihilation lifetime spectroscopy
PC	Polycarbonate
PMMA	Polymethylmethacrylate
PU	Polyurethane
PVB	Polyvinyl butyral
Sapphire	Single-crystal aluminium oxide (Al_2O_3)
SEC	Size exclusion chromatography
SEM	Scanning electron microscopy
SENB	Single edge-notched three point bend
SHPB	Split Hopkinson pressure bar
SHTB	Split Hopkinson tension bar
Spinel	Magnesium aluminate ($MgAl_2O_4$)
T_g	Glass transition temperature
TPU	Thermoplastic polyurethane
TTS	Time-temperature superposition

T_α	α-relaxation temperature (same as the glass transition temperature, T_g)
T_β	β-relaxation temperature
UV	Ultraviolet
VIS	Visible
V_{50}	Ballistic limit velocity

References

[1] T. Eshel, "Advances in Transparent Armor Improving Vision from Armored Vehicles", Defence Update, 29 May 2017. Online: https://defense-update.com/20170529_transparent_armor.html

[2] E. Yang, S. Cimpoeru, P. Phillips, "Effect of Environmental Aging on the Ballistic Performance of Transparent Armour – An Experimental Study", in *Workshop on ageing effects in protective systems, components and materials*, Saint-Louis, France, 4-5 April 2017.

[3] M. C. Henry, "Chapter 5 - Transparent Armor", in *Methods and Phenomena Ballistic Materials and Penetration Mechanics*, R. C. Laible Ed., 5. ed.: Elsevier, 1980, pp. 117-134.

[4] P. J. Patel, G. A. Gilde, P. G. Dehmer, J. W. McCauley, "Transparent Armor", in *The AMPTIAC Newsletter*, vol. 4, no. 3, ed. Rome, New York, USA: Advanced Materials and Processes Technology, AMPTIAC, 2000, pp. 1-13.

[5] M. J. Sands, P. J. Patel, P. G. Dehmer, A. J. Hsieh, M. C. Boyce, "Protecting the Future Force: Transparent Materials Safeguard the Army's Vision", in *The AMPTIAC Quarterly*, vol. 8, no. 4, ed. Rome, New York, USA: Advanced Materials and Processes Technology, AMPTIAC, 2004, pp. 28-36.

[6] M. Grujicic, W. C. Bell, B. Pandurangan, "Design and material selection guidelines and strategies for transparent armor systems", *Materials & Design,* vol. 34, pp. 808-819, 2012.

[7] J. M. Sloan, P. Patterson, "Mechanisms of Photo Degradation for Layered Silicate-Polycarbonate Nanocomposites", Army Research Laboratory, Aberdeen Proving Ground, Maryland, USA, ARL-TR-3649, 2005.

[8] I. G. Crouch, J. Sandlin, S. Thomas, "Polymer and fibre-reinforced plastics", in *The Science of Armour Materials*, I. G. Crouch Ed. London, UK: Woodhead Publishing, 2017, ch. 5, pp. 203-268.

[9] "Opportunities in protection materials science and technology for future army applications", Washingon DC, USA: The National Academies Press, 2011.

[10] I. G. Crouch, G. V. Franks, S. Thomas, M. Naebe, "Glasses and ceramics", in *The Science of Armour Materials*, I. G. Crouch Ed. London, UK: Woodhead Publishing, 2017, ch. 7, pp. 331-393.

[11] E. Strassburger, "Ballistic testing of transparent armour ceramics", Journal of the European Ceramic Society, vol. 29, pp. 267-273, 2009.

[12] N. S. de Melo, R. P. Weber, J. C. M. Suarez, "Toughness behavior of gamma-irradiated polycarbonate", *Polymer Testing,* vol. 26, no. 3, pp. 315-322, 2007.

[13] D. M. Martin, R. W. Lewis, G. W. Thomas, in *Army Sci. Conf. Proc.*, Cameron Station, Alexandria, Virginia, USA, 1968, vol. II.

[14] N. G. McCrum, C. P. Buckley, C. B. Bucknall, *Principles of Polymer Engineering*, 2 ed. Oxford, UK: Oxford University Press, 1997.

[15] T. A. P. Engels, L. C. A. van Breemen, L. E. Govaert, H. E. H. Meijer, "Criteria to predict the embrittlement of polycarbonate", *Polymer,* vol. 52, no. 8, pp. 1811-1819, 2011.

[16] M. E. J. Dekkers, D. Heikens, "The Tensile Behavior of Polycarbonate and Polycarbonate-Glass Bead Composites", *Journal of Applied Polymer Science,* vol. 30, no. 6, pp. 2389-2400, 1985.
[17] Q. H. Shah, Y. A. Abakr, "Effect of distance from the support on the penetration mechanism of clamped circular polycarbonate armor plates", *International Journal of Impact Engineering,* vol. 35, no. 11, pp. 1244-1250, 2008.
[18] A. Dwivedi, J. Bradley, D. Casem, "Mechanical Response of Polycarbonate with Strength Model Fits", Army Research Laboratory, Aberdeen Proving Ground, Maryland, USA, ARL-TR-5899, 2012.
[19] C. Bauwens-Crowet, J.-M. Ots, J.-C. Bauwens, "Strain-Rate and Temperature-Dependence of Yield of Polycarbonate in Tension, Tensile Creep and Impact Tests", *Journal of Materials Science,* vol. 9, no. 7, pp. 1197-1201, 1974.
[20] G. A. Adam, R. N. Haward, A. Cross, "Effect of Thermal Pretreatment on Mechanical-Properties of Polycarbonate", *Journal of Materials Science,* vol. 10, no. 9, pp. 1582-1590, 1975.
[21] A. Husain, R. Ansari, A. H. Khan, "Experimental and Numerical Investigation of Perforation of Thin Polycarbonate Plate by Projectiles of Different Nose Shape", *Latin American Journal of Solids and Structures,* vol. 14, no. 2, pp. 357-372, 2017.
[22] S. S. Sarva, M. C. Boyce, "Mechanics of polycarbonate during high-rate tension", *Journal of Mechanics of Materials and Structures,* vol. 2, no. 10, pp. 1853-1880, 2007.
[23] K. Cao, X. Z. Ma, B. S. Zhang, Y. Wang, Y. Wang, "Tensile behavior of polycarbonate over a wide range of strain rates", *Materials Science and Engineering A-Structural Materials Properties Microstructure and Processing,* vol. 527, no. 16-17, pp. 4056-4061, 2010.
[24] C. R. Siviour, S. M. Walley, W. G. Proud, J. E. Field, "The high strain rate compressive behaviour of polycarbonate and polyvinylidene difluoride", *Polymer,* vol. 46, no. 26, pp. 12546-12555, 2005.
[25] S. Q. Fu, Y. Wang, Y. Wang, "Tension testing of polycarbonate at high strain rates", *Polymer Testing,* vol. 28, no. 7, pp. 724-729, 2009.
[26] T. Hahn, N. Herzig, "Ageing of laminated glass – Characterization of Polycarbonate (PC) in aged and not aged condition at high strain rates", in *2nd Workshop on ageing effects in protective systems, components and materials*, Saint-Louis, France, 15-17 May 2018.
[27] A. J. Hill, K. J. Heater, C. M. Agrawal, "The Effects of Physical Aging in Polycarbonate", *Journal of Polymer Science Part B-Polymer Physics,* vol. 28, no. 3, pp. 387-405, 1990.
[28] A. D. Mulliken, M. C. Boyce, "Mechanics of the rate-dependent elastic-plastic deformation of glassy polymers from low to high strain rates", *International Journal of Solids and Structures,* vol. 43, no. 5, pp. 1331-1356, 2006.
[29] S. C. Wright, N. A. Fleck, W. J. Stronge, "Ballistic Impact of Polycarbonate - An Experimental Investigation", *International Journal of Impact Engineering,* vol. 13, no. 1, pp. 1-20, 1993.
[30] R. L. Woodward, S. J. Cimpoeru, "A study of the perforation of aluminium laminate targets", *International Journal of Impact Engineering,* vol. 21, no. 3, pp. 117-131, 1998,
[31] J. Radin, W. Goldsmith, "Normal Projectile Penetration and Perforation of Layered Targets", *International Journal of Impact Engineering,* vol. 7, no. 2, pp. 229-259, 1988.
[32] A. J. Hsieh, D. DeSchepper, P. Moy, P. G. Dehmer, J. W. Song, "The Effects of PMMA on Ballistic Impact Performance of Hybrid Hard/Ductile All-Plastic- and Glass-Plastic-

Based Composites", U.S. Army Research Laboratory, Aberdeen Proving Ground, Maryland, USA, ARL-TR-3155, 2004.
[33] L. Landi, A. Stecconi, F. Pera, E. Del Prete, C. Ratti, "Influence of the Shape Penetrator on Safety Evaluation of Machine Tools Guards", in *29th European Safety and Reliability Conference (ESREL)*, Hannover, Germany, 22-26 September 2019, pp. 2936-2943.
[34] Q. H. Shah, "Impact resistance of a rectangular polycarbonate armor plate subjected to single and multiple impacts", *International Journal of Impact Engineering,* vol. 36, no. 9, pp. 1128-1135, 2009.
[35] S. M. Walley, J. E. Field, P. W. Blair, A. J. Milford, "The effect of temperature on the impact behaviour of glass/polycarbonate laminates", *International Journal of Impact Engineering,* vol. 30, no. 1, pp. 31-53, 2004.
[36] A. Dorogoy, D. Rittel, A. Brill, "Experimentation and modeling of inclined ballistic impact in thick polycarbonate plates", *International Journal of Impact Engineering,* vol. 38, no. 10, pp. 804-814, 2011.
[37] Z. Rosenberg, R. Kositski, "Deep indentation and terminal ballistics of polycarbonate", *International Journal of Impact Engineering,* vol. 103, pp. 225-230, 2017.
[38] E. P. Carton, B. B. Johnsen, D. B. Rahbek, H. Broos, A. Snippe, "Round robin using the depth of penetration test method on an armour grade alumina", *Defence Technology,* vol. 15, no. 6, pp. 829-836, 2019.
[39] C. Lo, H. Li, G. Toussaint, J. D. Hogan, "On the evaluation of mechanical properties and ballistic performance of two variants of boron carbide", *International Journal of Impact Engineering,* vol. 152, p. 103846, 2021.
[40] A. Ram, O. Zilber, S. Kenig, "Life Expectation of Polycarbonate", *Polymer Engineering and Science,* vol. 25, no. 9, pp. 535-540, 1985.
[41] D. J. A. Senden, T. A. P. Engels, S. H. M. Sontjens, L. E. Govaert, "The effect of physical aging on the embrittlement of steam-sterilized polycarbonate", *Journal of Materials Science,* vol. 47, no. 16, pp. 6043-6046, 2012.
[42] E. S. Sherman, A. Ram, S. Kenig, "Tensile Failure of Weathered Polycarbonate", *Polymer Engineering and Science,* vol. 22, no. 8, pp. 457-465, 1982.
[43] S. Kahlen, G. M. Wallner, R. W. Lang, "Aging behavior and lifetime modeling for polycarbonate", *Solar Energy,* vol. 84, no. 5, pp. 755-762, 2010.
[44] T. Holmes, P. Phillips, T. O'Hara, S. J. Cimpoeru, "Long-term natural ageing of transparent armour in a high-temperature and high-humidity environment," in *4th Workshop on ageing effects in protective systems, components and materials*, Saint-Louis, France, 25-26 October 2022.
[45] R. Welker, S. Forster, T. Hofmann, "Testing and analysis of polymeric components and interfaces", in *2nd Workshop on ageing effects in protective systems, components and materials*, Saint-Louis, France, 15-17 May 2018.
[46] R. Balkova, T. Binar, J. Svarc, R. Mikulikova, P. Dostal, "The influence of temperature and cyclic loading on adhesion in polycarbonate-polyurethane-glass adhesive joint", *Journal of Adhesion Science and Technology,* vol. 33, no. 13, pp. 1381-1393, 2019.
[47] T. W. Loh, P. Tran, R. Das, R. B. Ladani, A. C. Orifici, "Thermoplastic polyurethane-cellulose nanocomposite for transparent armour: Characterisation of adhesion and thermal aging", *Composites Communications,* vol. 22, p. 100465, 2020.
[48] E. M. Pint, J. Fleming, G. Germanovich, L. Muggy, "Addressing Ballistic Glass Delamination in the Marine Corps Tactical Vehicle Fleet: Implications for Resourcing and Readiness", Santa Monica, California, USA: RAND Corporation, 2018.

[49] E. Carton, "Delamination of Transparent Armour Systems (TAS)", in *Workshop on ageing effects in protective systems, components and materials*, Saint-Louis, France, 4-5 April 2017.
[50] T. Parker, R. Welker, T. Hofmann, "Investigation of nano-layered vapor barriers for transparent armor", in *3rd Workshop on ageing effects in protective systems, components and materials*, Saint-Louis, France, 15-17 October 2019.
[51] R. Welker, S. Forster, T. Hofmann, T. Parker, "Transparent armor: Advances in the determination of aging effects", in *3rd Workshop on ageing effects in protective systems, components and materials*, Saint-Louis, France, 15-17 October 2019.
[52] R. Welker, T. Hahn, M. Güntner, "Transparent armor - high dynamic behavior of aged components", in *4th Workshop on ageing effects in protective systems, components and materials*, Saint-Louis, France, 25-26 October 2022.
[53] G. Rivers, A. Sirois, D. Cronin, "Influence of Moisture and Thermal Cycling on Delamination in Coupon Scale Glass-TPU-PC Transparent Armour Materials", in *3rd Workshop on ageing effects in protective systems, components and materials*, Saint-Louis, France, 15-17 October 2019.

About FFI

The Norwegian Defence Research Establishment (FFI) was founded 11th of April 1946. It is organised as an administrative agency subordinate to the Ministry of Defence.

FFI's mission

FFI is the prime institution responsible for defence related research in Norway. Its principal mission is to carry out research and development to meet the requirements of the Armed Forces. FFI has the role of chief adviser to the political and military leadership. In particular, the institute shall focus on aspects of the development in science and technology that can influence our security policy or defence planning.

FFI's vision

FFI turns knowledge and ideas into an efficient defence.

FFI's characteristics

Creative, daring, broad-minded and responsible.

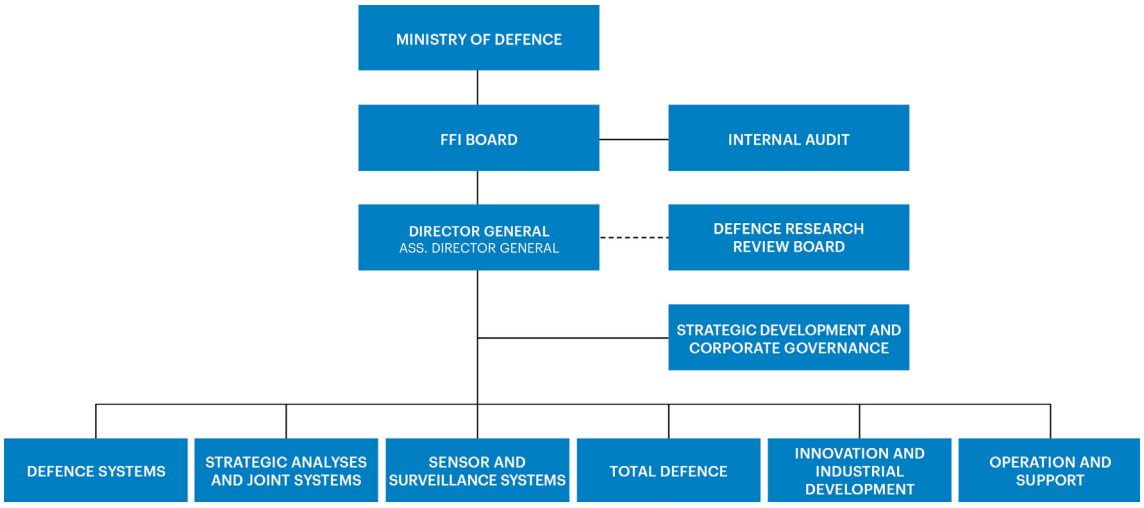

Forsvarets forskningsinstitutt (FFI)
Postboks 25
2027 Kjeller

Besøksadresse:
Kjeller: Instituttveien 20, Kjeller
Horten: Nedre vei 16, Karljohansvern, Horten

Telefon: 91 50 30 03
E-post: post@ffi.no
ffi.no

Norwegian Defence Research Establishment (FFI)
PO box 25
NO-2027 Kjeller
NORWAY

Visitor address:
Kjeller: Instituttveien 20, Kjeller
Horten: Nedre vei 16, Karljohansvern, Horten

Telephone: +47 91 50 30 03
E-mail: post@ffi.no
ffi.no/en